2nd round of response to referees:

Responses of sub-ice platelet layer thickening rate and frazil ice concentration to variations in Ice Shelf Water supercooling in McMurdo Sound, Antarctica

Chen Cheng, Adrian Jenkins, Paul R. Holland, Zhaomin Wang, Chengyan Liu, and Ruibin Xia

This response comprises Reply to Editor, Reply to Referee #1, Reply to Referee #2, and Reply to Referee #3. Each of our replies to the referees is structured as a sequence of comments from the referee, our response, and changes made to the manuscript.

Note: Italic denotes the referees' comments, and the following is our response. "P*L#" denotes line # in page * of the 'tracked changes' version of the manuscript in which blue characters exactly represent the revised part. Double quote represents the excerpt of the revised manuscript. Almost all the references mentioned in this report can be found in the **References** section of the manuscript; otherwise, we have given the full citation.

Reply to Editor:

Comments to the Author:
Dear authors,
thank you for the revisions of your manuscript which have now undergone another round of thorough reviews. I am glad to say that I agree that I find the manuscript publishable once the new, constructive reviewer's comments have been taken into account and implemented. I am grateful for having received such constructive comments and hope that you will be able to address and implement them almost 1:1. I am looking forward to receive your replies and revisions. Thank you and best regards
Christian Haas

Dear Editor Haas,

Thank you for your great support and encouragement for our manuscript. As you suggested, we have taken the new, constructive referees' comments into account and implemented them to our best ability. We hope to address all the specific issues below. In addition, we clarify that we have carefully checked for typos, missing co-authors and their affiliations, terminology, updates of data in tables, and updates of variables in equations.

Chen Cheng and other co-authors

Reply to Referee #1:

The authors have revised their manuscript and made significant improvements (including to the quality of the explanations and calculations of the suspension index). The topic of the paper is interesting and worthwhile. However, there remain some substantial issues with the paper, as summarized below. Therefore, I don't think the manuscript presently merits publication. With further changes, it could potentially be published in some journal in future.

We thank Referee #1 for his/her 2nd round of comments on our manuscript.

Major issues:

Novelty. The authors now do a better job explaining the novelty of their approach and the contribution of previous studies. However, it remains the case that this paper represents fairly incremental progress on their previous modelling paper. The particular geographical application is interesting but not totally compelling (the other reviewers raise important discrepancies between model and observations).

It was not our intention to develop the earlier model, but rather to apply it to a region where the observations, although still sparse, are the best available to validate the model output. Furthermore, we used the results to investigate the relationship between supercooling and SIPL growth. Therein lies the novelty of our paper. This is stated in the introduction:

"

McMurdo Sound therefore seems an ideal setting in which to apply and evaluate the new vertically-modified ISW plume model proposed by Cheng et al. (2017), which includes time dependence and two horizontal dimensions. The main objective is to explore possibility of finding the quantitative relationship between SIPL thickening rate and ISW supercooling.

"

and we have retained that wording (P3L1-3).

In terms of interpretation, the paper still does not make it clear why the suspension index should be relatively large (greater than one, say). I can only guess that the various velocities that go into u are very small. I could only see one of these velocities reported in Table 1. It is not clear how widely applicable this situation is. For example, if the ambient currents were (say) 0.1 m/s (10 times larger than the value in Table 1), Z* could be a factor of 10 smaller and the novel process modelled would not be that important. The wider significance of the work is therefore unclear.*

Very small Z_* is just the limiting case of our modification (Fig. 2), which is unlikely to occur in regions of active marine ice/SIPL formation. In our parameterization of frazil ice precipitation rate p' (Eq. 3),

$p' = w_i C_i \left(1 - \frac{U^2}{U_c^2}\right) \times He\left(1 - \frac{U^2}{U_c^2}\right)$,

the ratio of $\frac{U}{U_c}$ can be regarded as the reciprocal of Z_*, that is, $\frac{u_*}{w_i}$ (κ is dropped). Therefore, if Z_* is small, $\frac{U}{U_c}$ is large, which limits the precipitation. Therefore, in regions of high precipitation we would expect to find a non-uniform vertical distribution of frazil. We have added the following comment to the manuscript to clarify this point (P4L25-27):

"

While low values of Z_* are attainable with strong currents, those conditions also reduce the tendency for frazil to precipitate and contribute to SIPL formation [see Eq. (3) below]. Therefore, we expect a non-uniform vertical distribution of frazil wherever there is active formation of SIPL.

"

Correctness. A major issue relates to the choice of model parameters and the correctness of the numerical solution of the governing equations. In figure R, the authors present the results of calculations with a better-resolved discretization of the crystal size distribution. These differ markedly from the standard discretization presented in the paper, indicating that the standard results are inaccurate. A reader would not be aware of this important issue from the discussion on P6:L9-13. In their response, the authors argue that the poorly resolved discretization is better because it 'agrees' with observation. This argument is fallacious. Rather, the evidence suggests that there is some large flaw in another part of the model (most likely some choice of model parameters or, worse, some structural issue).

We apologize for a lack of clarity in our earlier response. We agree that the better agreement with observation using the less well resolved crystal size distribution must result from our choice of other parameter values. Those choices are consistent with earlier work (as we now clarify in response to reviewer 2), although most are poorly constrained. The point we were trying to make is that increasing the number of crystal size classes does not alter the results qualitatively (although it does increase the sensitivity to Z*). Therefore, if we were to rerun the models with a better-resolved crystal size distribution and parameters retuned to improve the fit between model results and observations, our conclusions would be the same. We prefer to stick with the simpler model and parameters choices closer to those used by others. To clarify this point we have added the following comment (P6L14-15):

"

Sensitivity experiments with more crystal size classes yielded qualitatively similar results.

"

The authors have not addressed the issue regarding the conversion of precipitation rate to ice thickening rate, where there are large uncertainties. While outside the scope of their model, this process greatly influences the comparison of the model with observations. I also think that the neglect of latent heat release during volume doubling violates energy conservation.

Post-depositional processes are beyond the scope of our study, but we have emphasised the importance of considering such processes by adding a citation to the work of Buffo et al (2019) (P7L5-6):

“

Coupling our VM model with a model focusing on the processes associated with platelet ice accretion within the sea ice (Buffo et al., 2018) would be necessary to improve on that rough estimate, but is beyond the scope of the present study.

”

; the associated latent heat release within SIPL should be considered within sea ice models such as that of Buffo et al. (2018). Furthermore, the majority of latent heat released within the sea ice will be lost to the atmosphere above rather than the ocean below.

Reply to Referee #2:

Summary

The revisions and corrections made to this manuscript have significantly improved both its interest to the community, and clarity for the reader. However, some of my original comments have not been adequately considered, and in my opinion, would need to be properly addressed (both in response to reviewers and by modifying the article text) before the manuscript is ready for publication.

We thank Referee #2 for his/her 2nd round of constructive comments, which have helped us to improve the clarity of our manuscript.

Specific points:

1. All references to 'temperature' should be changed to 'potential temperature' (assuming this is indeed the quantity used). For example, the text in P2-L15 was modified in response to Reviewer #1's comments, to support the author's assertion that temperature can be treated as vertically-uniform within the ISW plume. Unless the qualifier 'potential' is used, this is incorrect, and not supported by observations.

Revised as suggested

2. Distinction between applicability to crystal accretions beneath sea ice and ice shelves remains unclear. In their response to my review, the authors note that "Beneath the platelet ice layers the supercooling is produced by the pressure drop experience by ISW at it emerges from beneath an ice shelf and rise towards the sea surface, while regions of marine ice accretion beneath ice shelves have typically very low basal slopes." I completely agree with this, and am therefore puzzled as to why the authors seem reluctant to identify this difference to the reader. This is exactly the mechanistic driver that would allow the sub-ice boundary layers to behave differently.

I am not suggesting that the work (tested for platelet layers beneath sea ice, and potentially applied to marine ice layers beneath ice shelves) is invalid. However, I do think that a statement clarifying the differences between the regimes is necessary for the reader (and may protect the authors of the present study in the event that their model is naively applied to a regime for which it has not been validated). Specifically, the potential sources of divergence are:

a. The difference in basal slope is likely to result in the ISW plume existing much closer to the in-situ freezing temperature than is observed in McMurdo Sound, with the result that in-situ supercooling is likely to be much smaller (and potentially similar to the resolution of present-day instruments. i.e. unobservable except by implication) beneath ice shelves;

b. The difference in basal slope also has implications for generating buoyancy-induced momentum, which is the implicit source of the background current in Hughes et al. (2014), and therefore would need to be excluded (or vastly reduced) for application to an ice shelf cavity.

c. The authors allude to another difference with their statement "The one indirect effect on the ISW plume might be an increased drag coefficient beneath the platelet layer, where more rapid freezing of the deposited crystals may create more irregularity in the form of the ice-ocean interface." This is true, and will affect the sedimentation process.

d. In addition to the above, the length of time over which crystal accretion may occur is vastly different (i.e. about 1-3 years in McMurdo Sound vs tens-hundreds of years beneath ice shelves). Combined with the likely difference in degree of supercooling, this could potentially lead to very different internal structures of the crystal layers (e.g. marine ice layers more likely to collapse under accreted buoyancy), and hence present different physical boundaries to ocean flow, and an entirely different source of effective hydrodynamic drag (as suggested by Robinson et al., 2017, which the authors cite).

e. Finally, the observed supercooled plume in McMurdo Sound, having only recently experienced the step-change in pressure, is still adjusting to the change through active ice formation (onto both suspended frazil and to accreted platelet ice), and will therefore come to a point of equilibrium at some point beyond where the observations to date have been made. This represents a significantly different thermodynamic regime to the general situation of an ISW plume beneath an ice shelf.

This specifically relates to P11L8-10 of the revised manuscript, since in the general sub-ice shelf regime, the supercooled layer will almost certainly not approach the thickness observed in McMurdo Sound. This may have implications for the regime for which 'the efficiency of converting ISW supercooling into frazil concentration … is determined by the suspension index', since this is true only when 'the thickness of a supercooled layer of ISW is large enough' (P11L8-10) (i.e. greater than 65 m for the McMurdo Sound parameters).

I suggest that the addition of a well-crafted paragraph of text outlining the potential differences between the regimes would be sufficient to both demonstrate that the authors understand the implications of these differences (and I am convinced they do), and highlight to the reader where caution (and/or improved understanding) is required in applying this model to the sub-ice shelf regime.

Thank you for your very thorough discussion of this specific issue. We added more details as suggested (P12L10-25):

"

Results may differ from those discussed above, because of the subtly different environments beneath sea ice and ice shelves. Beneath a SIPL, supercooling is produced by the pressure drop experienced by ISW as it emerges from beneath an ice shelf and rises towards the sea surface, while supercooling that drives marine ice accretion beneath ice shelves is produced as the ISW ascends a very gentle basal slope. The in-situ supercooling level beneath ice shelves is therefore likely to be much smaller than that observed in McMurdo Sound, while the differing slopes also yield differing buoyancy forcing on the flow.

Furthermore, after experiencing the step-change in pressure as it ascends the ice front, the supercooled plume in McMurdo Sound is in the process of adjustment, through the formation of suspended frazil and direct freezing onto the accreted SIPL, towards an equilibrium that is presumably attained beyond the region of observations. At the base of an ice shelf, typically several hundred meters thick, the vertical temperature gradient is comparatively small, so the deposited crystals form a slushy layer (Engelhardt and Determann, 1987) that slowly consolidates, possibly as much through compaction as freezing. The ice-ocean interface and the associated drag coefficient are therefore likely to be very different to those observed in McMurdo Sound, where SIPL appears to comprise a more open matrix of ice and water that consolidates by freezing as heat is lost to the atmosphere. In addition, the vastly different time scales over which crystal accretion occurs (about 1-3 years in McMurdo Sound vs tens-hundreds of years beneath ice shelves) could lead to further differences in the internal structure of the crystal layers and hence in the physical boundaries they present to the ISW plume.

”

3. Justification for values of parameters used, and acknowledgement of available observations. In their response, the authors point to the lack of ‘observational guidance’ as justification for the extensive tuning of specific parameters. I agree, there are very little data available to constrain the models. However, the values they have chosen do find support in the literature, and it would strengthen the paper to acknowledge these. In particular (P7L9-10):

a. ISW outflow properties: the chosen values for temperature and salinity coincide with those reported by Hughes et al., 2014;

b. Platelet layer basal drag coefficient: the value chosen fits appropriately within the range identified by Robinson et al., 2017;

c. Frazil ice crystal size distribution: unknown, but presumably these are chosen from somewhere – perhaps previous modelling studies? Similarly for the Shields criterion?

d. Ambient current speed: The chosen value is consistent with the lowest speeds reported by Robinson et al., 2014 (although lower than their reported residual flow).

e. In addition, the observations in both Hughes et al. (2014) and Robinson et al. (2014) papers show the homogeneous ISW layer (observed in the centre of the modelled plume flow) as being 150 - 200 m thick, and the supercooled portion extending to 60/70 m. I would have thought these would be useful reference points for this manuscript.

Thank you for these useful comments. We added more details as suggested (P7L15-23):

“

Despite the limited observational constraints on many of these parameters we do find support in the literature for our adopted values: ISW outflow properties are consistent with those reported by HU14, and the corresponding thickness of supercooled layer is within the observed range (60-70 m) given in both HU14 and Robinson et al. (2014); the basal drag coefficient fits appropriately within the range identified by Robinson et al. (2017), while the ambient current speed is consistent with the lowest speeds reported in that study; we used 5 crystal size classes, as did Galton-Fenzi et al. (2012), although our sizes are slightly larger; we used a larger Shields criterion than the middle (0.05) of the observed range, although there is considerable scatter amongst the individual results reported from sedimentary experiments. Table 1 summarises all the values adopted for the key parameters.

”

4. My concern about the apparent resolution in figures 5 & 6 still stands: the separation of the contour lines, especially around the core of the plume, implies greater resolution than the model contains. A potential solution may be to plot only every second contour line.

As suggested, we halved the number of contour lines.

Reply to Referee #3

The paper is logically and clearly written. It describes the application of a two-dimensional ISW plume model to a set of observations of an ISW under sea ice. The results are an improvement over the model of Hughes et al (2014), particularly in terms of their two-dimensional nature that illustrates the Coriolis effect along the centre line of the plume. In addition the authors show (as naively might be expected) that the vertical distribution of supercooling and frazil concentration determine the growth of the sub-ice platelet layer.

We thank Referee #3 for his/her constructive comments that have helped us to improve our manuscript.

Comment 1: Some details of the process of formation of sea ice need to be outlined and are ignored in the paper. There are two consequences

(i) The term "platelet layer" is confusing. The term "sub-ice platelet layer" was coined by Gow et al (1998) and later authors for the high porosity layer that principally forms by accumulation of ice from the water column. I think the authors use "platelet layer" to mean this friable layer beneath the more consolidated "incorporated platelet ice". Incorporated platelet ice can be identified easily in an ice core by its crystal structure, but its other physical properties (salinity, porosity, permeability) are very similar to the usual columnar sea ice. It is formed by the freezing of the sub-ice platelet layer due to heat loss to the atmosphere. The term "platelet layer" could be understood to mean the sum of the incorporated platelet ice and the sub-ice platelet layer. In my view "sub-ice platelet layer" or "SIPL" (as in the original version) should be used to avoid confusion.

Gow, A. J., S. F. Ackley, J. W. Govoni, and W. F. Weeks (1998), Physical and structural properties of land-fast sea ice in McMurdo Sound, Antarctica, in Antarctic Sea Ice: Physical Processes, Interactions and Variability, Antarct. Res. Ser., vol. 74, edited by M. O. Jeffries, pp. 355–374, AGU, Washington, D. C., doi:10.1029/AR074p0355.

We agree with this point. First, we added a citation to Gow et al. (1998) where the phrase "sub-ice platelet layer" first occurs (P2L3). Second, the process by which the upper parts of the SIPL become incorporated into the sea ice has been described in the previous version of the manuscript (P2L4-6 in the new revised manuscript). Third, we have reverted to the use of the acronym SIPL instead of the term "platelet layer" in both text and figures.

(ii) The data used from HU14 is the "sub-ice platelet layer" thickness in November. However the top portion of this layer will have become incorporated into the consolidated sea ice above. Thus the value used will be an underestimate of the true value had the freezing due to heat loss to the atmosphere not taken place. Better agreement might be obtained between model and observation if the thickness of the incorporated platelet ice was included. There are some values of the

incorporated platelet ice thickness in HU14 (Fig 8b) but it would be better derived from Figs 2 & 3 and the Supplementary material of Langhorne et al (2015).

We admit the incorporation of SIPL into the sea ice adds additional uncertainty into the comparison of our simulated SIPL thickness with observations. However, the complex processes by which SIPL is incorporated into the sea ice cover are beyond the scope of our study. The assumption we make in converting frazil precipitation into SIPL thickness and our direct comparison of that result with measured SIPL thickness follow exactly the procedures of HU14. This seems the most consistent approach, although, as stated in the new revised manuscript (see P6L31-P7L6), we believe that this issue would be potentially improved by coupling with specific sea ice models focusing on microscale processes within the bottom layer of the ice, such as Buffo et al. (2018).

Comment 2: The authors have conducted a significant sensitivity study. I would like to know what can be learned from this sensitivity study about the physics controlling the process of deposition of ice crystals; and how could this inform the design of observational campaigns. For example Fig 6 shows much steeper gradients in sub-ice platelet layer thickness than demonstrated in the observations. Why? Could there be post-depositional processes taking place that are not accounted for in the model; or a mismatch in the deifnition of between modeled and observed "platelet layer" (see next comment) or undersampling of the observations.

The authors are rather glib in simply saying that small scale features were not resolved by relatively coarse scale spatial distribution of the sea ice thickness measurements (incidently these were not ice core samples). Experimental evidence of steep gradients in the sub-ice platelet layer thickness have been published (Hunkeler et al, 2015) but these were associated with a sea ice breakout and an abrupt change in sea ice plus snow thickness. A significant change in sea ice thickness was not observed in the McMurdo Sound observations.

Hunkeler, P. A., M. Hoppmann, S. Hendricks, T. Kalscheuer, R. Gerdes (2016), A glimpse beneath Antarctic sea ice: Platelet layer volume from multifrequency electro- magnetic induction sounding, Geophys. Res. Lett., 43, 222–231, doi:10.1002/2015GL065074.

Further if the position of the 3 km wide plume outflow (an unknown in the model) was moved east or west by a small amount then there would be a big discrepancy between model and experiment.

The main purpose of conducting the extensive sensitivity runs was to reveal a comprehensive area-averaged relationship between SIPL thickening rate (i.e., the process of deposition of ice crystals) and ISW supercooling in McMurdo Sound, and that was shown to be predominantly controlled by the suspension index. Therefore, we highlight the need to improve the detection technology for suspended ice crystals within the sub-ice oceanic boundary layer. Referring to the steep gradient of SIPL thickness, HU14 also obtained a comparable gradient, that is, a decrease from 17 to 9 m (15 to 6 m in this study) within 5 km of the outflow (HU14, Fig. 10e). We have now expanded on the possible reasons why simulated gradients might be greater than observed ones (P8L25-P9L4):

“

The simulated SIPL thickness near the ISW outflow exhibits steeper gradients than are observed (Fig. 6b and c), which probably result from the spatial non-uniformity of ISW plume near the outflow (Fig. 5a and b). That non-uniformity in flow leads to localized non-uniformities in thermodynamics (Fig. 5c and d), frazil concentration (Fig. 5e and f), and thus SIPL thickness (Fig. 6b and c). Moreover, because the sea ice base is horizontal, there are no changes in the freezing point associated with pressure change, so supercooling is always highest at the ISW outflow (Fig. 5c and d). That results in the greatest frazil concentration (Fig. 5e and f) and SIPL thickness (Fig. 6b and c) near the location of the outflow, and because the outflow is steady in time spatial gradients in SIPL close to the outflow are enhanced. In reality, temporal changes in the ISW outflow position, width, supercooled layer thickness and duration could lead to a broader region of elevated frazil precipitation and a less peaked distribution of SIPL thickness. In addition, such small-scale features in the SIPL thickness distribution, if present, would not be resolved by the relatively coarse spatial distribution of drill-hole measurements (dots in Fig. 6). Nevertheless, the largest SIPL thickness undoubtedly occurs adjacent to the ISW outflow in McMurdo Sound, and the SIPL thickness calculated by the VM model at drill sites agrees well with the measurements (Fig. 6a), being graded “excellent” in contrast with the “poor” performance of the VU model (Table 2).

”

We also revised the text (P6L5-6) as “The initial thickness of the ISW outflow (indicated by blue arrow in Fig. 1) from underneath McMurdo Ice Shelf …” to clarify the position of the ISW outflow, and used the phrase “drill-hole measurements” instead of ice core samples after scrutinizing HU14 and Price et al. (2014) (Price, D., Rack, W., Langhorne, P. J., Haas, C., Leonard, G., and Barnsdale, K.: The sub-ice platelet layer and its influence on freeboard to thickness conversion of Antarctic sea ice, The Cryosphere, 8, 1031-1039, https://doi.org/10.5194/tc-8-1031-2014, 2014.). The latter utilized the same data sets as in HU14 and the present study.

Comment 3: Fig 1 is incorrect. A pre-2011 ice shelf front has been used and this means that the purple box has been placed too far to the north. The samples stations (red dots) are in the wrong locations.

Thank you for this correction. We have relocated the purple box and sample stations (red dots) completely following Figs. 6 and 9 in HU14.

Technical Corrections

p. 2, line 15-24: I was surprised that the instabilities derived by Jordan et al (2014) were not discussed in relation to the vertical distribution of frazil. Are they not relevant?

Jordan et al. (2014) (Jordan, J. R., Kimura, S., Holland, P. R., Jenkins, A., and Piggott, M. D.: On the conditional frazil ice instability in seawater, J. Phys. Oceanogr., 45, 1121-1138, http://doi.org/10.1175/JPO-D-14-0159.1, 2015) used a non-hydrostatic ocean model to study the conditional frazil ice instability during the rise of frazil ice from a depth of several hundred metres to the sea surface, while this study is focused on depth-integrated sub-ice ISW plume modelling that considers an equilibrium vertical distribution of frazil concentration within the plume. Therefore, although both studies are associated with frazil ice processes, they are not closely-related.

p. 3, Line 2-3: "The main objective is to quantify for the first time the response of the platelet layer thickening rate to variations in ISW supercooling." I don't think this can be claimed as a first as HU14 considered supecooling and sub-ice platelet layer thickness, as did Buffo et al (2018). Please delete "for the first time"

p. 8, line 26-30: "we know of no studies to date of the response of marine ice (or platelet layer) thickening rate beneath ice shelves (or sea ice) to variations in supercooling," Again I would argue that HU14 and Buffo et al (2018) considered this relationship.

We admit that both HU14 and Buffo et al. (2018) focused on the issue of SIPL growth from supercooled water, but neither explored the quantitative relationship between ISW supercooling and SIPL thickening rate. We have edited the sentences to clarify the novel aspect of our study:

"

The main objective is to explore possibility of finding the quantitative relationship between SIPL thickening rate and ISW supercooling.

" (P3L2-3).

"

In contrast, we know of no studies to date that provide a quantitative relationship between marine ice (or SIPL) thickening rate beneath ice shelves (or sea ice) and ISW supercooling. Such a relationship is of potential significance for evaluating the mass balance of deep-draughting ice shelves in cold water environments and adjacent sea ice subject to climatic variability.

" (P9L15-18).

p. 8, line 13-18: The authors are rather glib in simply…there would be a big discrepancy between model and experiment.

See the above response to Comment 2.

On the other hand I think the authors could expand on the relationship and provide insights and explanations.

p. 10, line 21-26: This is exactly the sort of explanation that I find a useful outcome of the detailed modeling.

The relationship is rather complex, and we have attempted to offer insight through our choice of Figures. Fig. 7a depicts the relationship between ISW supercooling and thickening rate as a function of supercooling of the outflow, indicating two critical supercooling levels dividing the relationship into three regimes. Fig. 7b demonstrates that this complexity stems from the suspension index. Fig. 8 further illustrates the control of suspension index on the efficiency with which the supercooling is utilized. Fig. 10 more explicitly presents the control of suspension index on the thickening rate and frazil concentration. Subsections 4.2 and 4.3 discuss these figures in detail.

Responses of sub-ice platelet layer thickening rate and frazil ice concentration to variations in Ice Shelf Water supercooling in McMurdo Sound, Antarctica

Chen Cheng[1,2,3], Adrian Jenkins[2], Paul R. Holland[2], Zhaomin Wang[4], Chengyan Liu[4,1,3], and Ruibin Xia[1,3]

[1]Polar Climate System and Global Change Laboratory, Nanjing University of Information Science & Technology, Nanjing, 210044, China
[2]British Antarctic Survey, Cambridge, CB3 0ET, UK
[3]School of Marine Sciences, Nanjing University of Information Science & Technology, Nanjing, 210044, China
[4]College of Oceanography, Hohai University, Nanjing, 210098, China

Correspondence to: Zhaomin Wang (zhaomin.wang@hhu.edu.cn)

Abstract. Persistent outflow of supercooled Ice Shelf Water (ISW) from beneath McMurdo Ice Shelf creates a rapidly growing sub-ice platelet layer (SIPL) having a unique crystallographic structure under the sea ice in McMurdo Sound, Antarctica. A vertically-modified frazil-ice-laden ISW plume model that encapsulates the combined nonlinear effects of the vertical distributions of supercooling and frazil concentration on frazil ice growth is applied to McMurdo Sound, and is shown to reproduce the observed ISW supercooling and SIPL distributions. Using this model, the dependence of SIPL thickening rate and depth-averaged frazil ice concentration on ISW supercooling in McMurdo Sound is investigated, and found to be predominantly controlled by the vertical distribution of frazil concentration. The complex dependence on frazil concentration highlights the need to improve frazil ice observations within the sea ice-ocean boundary layer in McMurdo Sound.

1 Introduction

Ice shelf basal melting removes more mass from the Antarctic Ice Sheet than iceberg calving does, but the three largest ice shelves, Filchner-Ronne, Ross, and Amery, contribute only 18% of the net meltwater flux (Rignot et al., 2013). That is because the seawater-filled cavities beneath those ice shelves are dominated by High Salinity Shelf Water that has a potential temperature at or near the surface freezing point. Ice shelf basal melting occurs at depth, because the freezing point temperature is lower under elevated pressure, and results in the formation of Ice Shelf Water (ISW), characterized by potential temperatures below the surface freezing point. When the buoyant ISW ascends along the ice shelf base, the pressure relief causes it to become supercooled in situ, a necessary condition for ice crystals to persist in suspension. Those disk-shaped frazil ice crystals accumulate under the ice shelves, leading to the formation of marine ice that is thicker and more localized than would be possible through direct freezing at the ice shelf base (Morgan, 1972; Oerter et al. 1992; Fricker et al., 2001; Holland et al., 2007, 2009). Occasionally, frazil ice crystals bathed in supercooled ISW are also carried out beyond the ice shelf front and precipitated under adjacent sea ice, forming an unconsolidated, porous, sub-ice platelet layer (SIPL) (Gow et al., 1998; Hunkeler et al., 2016; Langhorne et al., 2015; Leonard et al., 2006; Robinson et al., 2014). SIPL not only harbours some of the highest concentrations of sea ice algae on Earth (Arrigo et al., 2010) but also contributes to the sea ice thickness when the water within the pores of SIPL freezes, due to heat loss to the atmosphere, to become incorporated platelet ice (Smith et al, 2001). Therefore, SIPL should not be ignored when investigating sea ice thickness near an ice shelf front.

Owing to the paucity of direct observation, our understanding of the evolution of frazil-ice-laden ISW relies heavily on numerical models. Those models are mostly derived from plume theory (Holland and Feltham, 2006; Jenkins and Bombosch, 1995; Rees Jones and Wells, 2018; Smedsrud and Jenkins, 2004), but include three-dimensional ocean circulation models (Galton-Fenzi et al., 2012), and have been widely applied to assess the marine ice beneath Filchner-Ronne (Bombosch and Jenkins, 1995; Holland et al., 2007; Smedsrud and Jenkins, 2004), Larsen (Holland et al., 2009) and Amery ice shelves (Galton-Fenzi et al., 2012), and SIPL under the sea ice in McMurdo Sound (Hughes et al., 2014, hereinafter HU14). To date, all the ISW plume models mentioned above have been depth-integrated, and all the scalar quantities, i.e., potential temperature, salinity, and frazil concentration in those models are treated as vertically-uniform. The well-mixed potential temperature and salinity have been validated by borehole observations beneath the Amery Ice Shelf (Herraiz-Borreguero et al., 2013) and under the sea ice in McMurdo Sound (Robinson et al., 2014; HU14). Although there are no observations of the vertical profile of frazil ice concentration, it is unlikely to be vertically uniform because the buoyant rise of the crystals will counteract the turbulent diffusion that tends to homogenise the other properties. Recently, Cheng et al. (2017) showed that adopting an approach in which the frazil ice growth is calculated using a vertically-uniform frazil concentration results in substantial underestimation of marine ice production underneath the western side of Ronne Ice Shelf. Idealized one dimensional models confirm that the vertical distribution of frazil concentration cannot remain well-mixed in the upper layers of the ocean (Svensson and Omstedt, 1998) and beneath ice shelves (Holland and Feltham, 2005). Consequently, earlier assessments of either marine ice or SIPL production in the aforementioned areas may need to be re-evaluated.

McMurdo Sound, located in the southwestern Ross Sea (Fig. 1), is characterized by significant ISW outflow, arguably one of the most comprehensively observed ISW plumes available (HU14; Langhorne et al., 2015; Robinson et al. 2014). A prominent SIPL forms in the central-western sound (Dempsey et al., 2010); the maximum (area-averaged) observational first-year sea ice and SIPL are 2.5 (2) and 8 (3) m as determined from drill-hole measurements adjacent to McMurdo Ice Shelf front between late November and early December in 2011 (Fig. 9 in HU14). The thin (~20 m) McMurdo Ice Shelf front allows the ISW outflow to be delivered to the ocean surface without mixing with warmer ambient waters (Robinson et al., 2014). The study documented in HU14 was the first to apply the steady, one-dimensional frazil-ice-laden ISW plume model developed by Smedsrud and Jenkins (2004) to McMurdo Sound, although a constant ISW plume thickness was used.

McMurdo Sound therefore seems an ideal setting in which to apply and evaluate the new vertically-modified ISW plume model proposed by Cheng et al. (2017), which includes time dependence and two horizontal dimensions. The main objective is to explore possibility of finding the quantitative relationship between SIPL thickening rate and ISW supercooling. Establishing such a relationship is of significance to the assessment of total sea ice thickness, and thus the oceanic heat flux associated with SIPL, in McMurdo Sound and elsewhere.

Here we first analyze the combined nonlinear effects of the vertical distributions of supercooling and frazil concentration on the suspended frazil ice growth rate in a supercooled ISW plume, and compare results with those obtained with a commonly-used, depth-averaged formulation. Then, we evaluate the performance of the vertically-modified ISW plume model in reproducing the observed ISW supercooling and SIPL distribution to show the importance of considering the combined nonlinear effects. Finally, we conduct 211 sensitivity simulations with the purpose of quantitatively establishing the response of SIPL thickening rate as well as the frazil ice concentration to variations in ISW supercooling in McMurdo Sound.

2 Physically-based formulation for frazil ice growth rate

The growth rate of suspended frazil ice controls both the dynamic and thermodynamic evolution of ISW plumes and the accretion of ice crystals beneath ice shelves (Cheng et al., 2017; Holland and Feltham, 2006; Smedsrud and Jenkins, 2004) and sea ice (HU14). The frazil ice growth rate is found to be proportional to the following integral expression once a number of physical parameters within the commonly-used formulation of Jenkins and Bombosch (1995) are merged:

$$I_{gr} = \int_0^1 T_{SC}\, c_i(\sigma) d\sigma, \quad T_{SC} = T_f(\sigma, S) - T, \tag{1}$$

where $\sigma \in [0, 1]$ is the relative vertical coordinate, with 0 and 1 respectively corresponding to the upper ice-plume and lower plume-ambient water interfaces, T and S are respectively the plume's potential temperature and salinity, vertically well-mixed within the plume, c_i is the vertically-distributed, in this study, volumetric frazil concentration within the plume, T_{SC} and T_f are respectively the supercooling level (positive for supercooling) and local freezing point. Because of the well-known linear decrease in T_f with increasing water depth, T_{SC} also varies linearly with depth, transitioning from supercooling to overheating as σ increases (Figs. 2a and 3). The corresponding transition height at which $T_{SC} = 0$ is defined by supercooled thickness $D_{SC} = \sigma_{SC} D$ where σ_{SC} and D are respectively supercooled fraction and total ISW plume thickness.

In earlier ISW plume models, because c_i is treated as vertically-uniform, the integral of (1) can be represented by the product of the depth-averaged values $T_{SC}^{0.5}$ (0.5 means at mid-depth) and C_i. Thus, we refer to these ISW plume models as vertically-uniform (VU). It is worth mentioning that in order to take the supercooling into account when σ_{SC}<0.5, HU14 integrated T_{SC} over the supercooled part only without introducing any frazil ice melting. However, in this study, we will demonstrate that the important role of frazil ice melting in the lower, overheated part of the plume cannot be ignored.

The vertical distribution of frazil concentration, in reality, much like the concentration of suspended sediment (Cheng et al., 2013, 2016), should be vertically non-uniform, with higher concentrations near the ice shelf/sea ice base. Considering only the balance between the buoyant-rise-induced vertical advection and turbulent diffusion terms, the governing equation for frazil concentration can be written as

$$\frac{d}{d\sigma}\frac{K}{D}\frac{dc_i}{d\sigma} + w_i\frac{dc_i}{d\sigma} = 0,$$

where w_i is the frazil ice rise velocity, determined by ice crystal size, K is the vertical frazil concentration diffusion coefficient, which can be parameterized as vertically constant (Cheng et al., 2013, 2016):

$$K = \frac{1}{6}\kappa u_* D,$$

where $\kappa = 0.4$ is von Karman's constant, $u_* = \sqrt{C_d}U$ is the friction velocity, related to the turbulent intensity within the ISW plume, C_d is the basal drag coefficient, $U = \sqrt{(U_p + U_a)^2 + (V_p + V_a)^2 + U_t^2}$ is the total flow speed, $U_p(U_a)$ and $V_p(V_a)$ are the depth-averaged ISW plume (ambient current) speed in the x and y directions respectively, U_t is the root-mean square tidal speed. Using a zero net flux condition in the equilibrium state at the lower boundary of the plume, i.e.,

$$\frac{K}{D}\frac{dc_i}{d\sigma} + w_i c_i = 0, \text{ for } \sigma=1$$

and a Dirichlet boundary condition at the upper boundary, i.e.,

$$c_i = c_{i,b}, \text{ for } \sigma=0$$

where $c_{i,b}$ is the frazil concentration at the ice shelf/sea ice base, the vertical exponential profile for the equilibrium frazil concentration can be readily obtained (Cheng et al., 2017):

$$\frac{c_i(\sigma)}{c_{i,b}} = exp(-6Z_*),$$

where $Z_* = w_i/\kappa u_*$ is the suspension index, otherwise known as the Rouse number. Integrating this exponential profile from σ=0 to 1, we finally obtain the relation between $c_i(\sigma)$ and C_i as

$$\frac{c_i(\sigma)}{C_i} = \frac{6Z_* exp(-6Z_*\sigma)}{1-exp(-6Z_*)}. \quad (2)$$

As shown in Fig. 2a, the vertical distribution of frazil concentration is strongly controlled by Z_*. The gradient of the vertical distribution becomes greater with increasing Z_*, and a vertically-uniform frazil concentration distribution can only be achieved as Z_* approaches 0. While low values of Z_* are attainable with strong currents, those conditions also reduce the tendency for frazil to precipitate and contribute to SIPL formation [see Eq. (3) below]. Therefore, we expect a non-uniform vertical distribution of frazil wherever there is active formation of SIPL. Accordingly, Cheng et al. (2017) introduced (2) into (1), and as a result significantly improved the simulated pattern of marine ice growth under the western side of Ronne Ice Shelf, compared with the VU and satellite-derived (Joughin and Padman, 2003) results. Hereinafter, we refer to this vertically-modified ISW plume model as VM. To conclude, the only difference between VM and VU models is whether the vertical distribution of frazil ice concentration is introduced.

The dependence of the integral value of I_{gr} on Z_* under specified conditions of supercooling (Fig. 2a) is shown in Fig. 2b, where $D_{SC} = 50$ m (a value within the calculated range for the standard run, Fig. 1) in all the cases. It can be seen that the integral value increases nonlinearly with Z_*. The critical Z_* that represents the transition from frazil ice melting ($I_{gr} < 0$) to freezing ($I_{gr} > 0$) decreases as the supercooled part of ISW plume increases. In contrast, owing to the neglect of vertical variation in c_i, the integral values calculated using the VU formulation are constant, leading to transitions from overestimation of frazil ice growth to underestimation, compared with VM, as Z_* increases. Only if the ISW plume is fully supercooled ($\sigma_{SC} = 1$) and Z_* is close to 0 are the integral values of I_{gr} calculated by VU and VM formulations equal (star in Fig. 2b). These features are illustrated in Fig. 2a: for given supercooling, if Z_* becomes larger, there is higher (lower) frazil concentration in the upper (lower), supercooled (overheated) part of the ISW plume. Owing to the assumption that thermohaline exchanges between frazil crystals and ambient water occur only at the crystal edge for freezing, but over the whole crystal surface for melting (Jenkins and Bombosch, 1995), the integral values of I_{gr} for the lower overheated part can be of much greater magnitude (Fig. 2b). It is therefore necessary to limit the mass loss due to frazil melting in one model time step such that it does not exceed the frazil concentration in the lower, overheated part of the plume. Overall, the frazil concentration and frazil growth rate distributions in the VM model show physically-reasonable and desirable characteristics that are absent from the VU model, and the impacts will be demonstrated by evaluation of the VM model in McMurdo Sound.

3 ISW model in McMurdo Sound

The unsteady VM and VU models used in this study are described in detail by Cheng et al. (2017). The governing equations for ISW properties and frazil concentration in both VM and VU models remain as they were in the depth-integrated, two-dimensional ISW plume model developed by Holland and Feltham (2006), except for the different treatments of the specific terms associated with the frazil ice growth rate, described above, in the frazil concentration and potential temperature transport equations of the VM model. Both VM and VU models combine the same commonly-used parameterizations of thermohaline exchanges across the ice–water interfaces, specifically a three-equation formulation (Holland and Jenkins, 1999) for the sea ice base and a two-equation formulation for frazil ice (Galton-Fenzi et al., 2012), with a multiple size–class frazil dynamics model (Smedsrud and Jenkins, 2004), to calculate basal freezing (f') and frazil melting/freezing (w'), secondary nucleation (N'), and precipitation (p'). These processes are summarized in Fig. 3. Rather than repeat all the equations here, we recall some of them and present how we set up our ISW plume models on the McMurdo Sound domain.

The model domain (Fig. 1) is delimited by a 45×40 km rectangle in the *x-y* plane with an ISW outflow from beneath McMurdo Ice Shelf. The base of the sea ice in McMurdo Sound is assumed to be horizontal and rough, owing to the presence of SIPL. The drag coefficient of the ice underside is therefore 6-30 times larger than that typically applied in ice-ocean interaction models (Robinson et al, 2017). The parameterization of the sea ice thermodynamics, the assumption of no entrainment of ambient water into the ISW plume, and the boundary conditions at the ISW outflow follow HU14. The initial thickness of the ISW outflow (indicated by blue arrow in Fig. 1) from underneath McMurdo Ice Shelf is set equal to that of the supercooled layer, i.e., $D = D_{SC}$, and the discharge per unit width is set to 0.02 m^2 s^{-1}. The addition of both an ambient circulation and tides follow HU14: the former, which represented the only source of momentum in the study of HU14, is assumed to be parallel to the Victoria Land coast, in the negative *y* direction, and to be constant throughout the model domain; the latter is calculated using root-mean square tidal speeds from Padman and Erofeeva (2005). Because ISW persists in McMurdo Sound for at least the 8-9 months of the ice growth season (Robinson et al., 2014), all runs are integrated for 240 days. The model resolution and time step ($\triangle t$) are 1 km and 25 s, respectively. The frazil ice size distribution is represented by 5 crystal size classes, and the transfer processes, induced by frazil freezing and melting, between different size classes are calculated using the scheme proposed by Smedsrud and Jenkins (2004). Sensitivity experiments with more crystal size classes yielded qualitatively similar results. The ice concentration at the ISW outflow is evenly distributed among the classes (Holland and Feltham, 2005, 2006; Smedsrud and Jenkins, 2004).

We treat the frazil ice precipitation rate p' as inverted sedimentation and follow the parameterization of McCave and Swift (1976):

$$p' = w_i C_i \left(1 - \frac{U^2}{U_c^2}\right) \times He\left(1 - \frac{U^2}{U_c^2}\right), \quad (3)$$

where U_c is a critical velocity, above which precipitation cannot occur, determined by Jenkins and Bombosch (1995):

$$U_c^2 = \frac{\theta_i(\rho_0 - \rho_i) g 2 r_e}{\rho_0 C_D},$$

where θ_i is the Shields criterion, ρ_0 and ρ_i are reference seawater and ice densities, respectively, g is gravity, r_e is the equivalent radius of a sphere with the same volume as the frazil disk. The frazil ice rise velocity, w_i, is calculated by Morse and Richard (2009):

$$w_i = \begin{cases} 2.025 D_i^{1.621} & if\ D_i \le 1.27\ mm \\ -0.103 D_i^2 + 4.069 D_i - 2.024 & if\ 1.27 < D_i \le 7\ mm \end{cases},$$

where $D_i = 2r_i$ is the diameter of a frazil crystal in mm. The inclusion of the Heaviside function He means that negative precipitation (i.e., erosion of previously deposited frazil ice) is not permitted. Because we have no idea about how cohesive the ice crystals are once they have settled, the estimation of an erosion rate would entail additional uncertainties.

The complex processes after the frazil ice precipitates onto the sea ice base are simplified in our model. In order to calculate SIPL thickness D_P at the n^{th} time interval, we adopt the assumptions of HU14 that solid ice fraction within SIPL in

McMurdo Sound is 0.25 based on the observational estimation from Gough et al. (2012) and that the ice crystals, on average, double in volume after precipitation:

$$D_P = \frac{1}{0.25} \times 2 \times \sum_{k=1}^{n} (p'_k \times \triangle t).$$

It should be noted that the volume change factor is a broad estimate, with almost no supporting evidence in the literature to guide it. Coupling our VM model with a model focusing on the processes associated with platelet ice accretion within the sea ice (Buffo et al., 2018) would be necessary to improve on that rough estimate, but is beyond the scope of the present study.

4 Results

4.1 Standard model run

The performance of the VU and VM models in reproducing the ISW supercooling and SIPL pattern in McMurdo Sound is evaluated by comparing results with observational data. To our knowledge, the data reported by HU14 are the most comprehensive available to evaluate our model, including both oceanographic and drill-hole measurements in two horizontal dimensions adjacent to McMurdo Ice Shelf. As this study represents the first application of a two-dimensional ISW plume model to the McMurdo Sound region, extensive tuning of the least constrained model parameters, including the ISW outflow properties, SIPL basal drag coefficient, frazil ice crystal size distribution, ambient current speed, and Shields criterion was required to produce the distributions of ISW properties and SIPL thickness shown in Figs. 4a and 6, respectively. Despite the limited observational constraints on many of these parameters we do find support in the literature for our adopted values: ISW outflow properties are consistent with those reported by HU14, and the corresponding thickness of supercooled layer is within the observed range (60-70 m) given in both HU14 and Robinson et al. (2014); the basal drag coefficient fits appropriately within the range identified by Robinson et al. (2017), while the ambient current speed is consistent with the lowest speeds reported in that study; we used 5 crystal size classes, as did Galton-Fenzi et al. (2012), although our sizes are slightly larger; we used a larger Shields criterion than the middle (0.05) of the observed range, although there is considerable scatter amongst the individual results reported from sedimentary experiments. Table 1 summarises all the values adopted for the key parameters. Model results are evaluated by means of skill metrics: Root-Mean-Square Error (RMSE), Correlation Coefficient (CC), and Skill Score (SS), respectively given by

$$RMSE = \left[\frac{\sum (X_{cal} - X_{obs})^2}{M}\right],$$

$$CC = \frac{\sum (X_{cal} - \overline{X_{cal}})(X_{obs} - \overline{X_{obs}})}{[\sum (X_{cal} - \overline{X_{cal}})^2 \sum (X_{obs} - \overline{X_{obs}})^2]^{1/2}},$$

$$SS = 1 - \frac{\sum (X_{cal} - X_{obs})^2}{\sum (X_{obs} - \overline{X_{obs}})^2},$$

where X is the variable being evaluated, M is the number of data points, and the overbar denotes the arithmetic mean. The performance of each model is indicated by SS as: >0.65 excellent; 0.65–0.5 very good; 0.5–0.2 good; <0.2 poor (Luo et al., 2017; Ralston et al., 2010; Song and Wang, 2013).

It can be seen that at the end of the simulations both VM and VU models reproduce the observed reduction in ISW supercooling at the sea ice base (T_{SC}^{0}, superscript "0" denotes the sea ice base) in the cross- and long-sound directions, in spite of some evident model discrepancies (Fig. 4a) that may result from the limitations in our model setup: both the ambient current and tides are treated as temporally and spatially constant; there are no long-term observations of ISW outflow to provide reliable boundary conditions; we use a constant drag coefficient, ignoring the spatiotemporal evolution of the sea ice basal form characterized by SIPL. We also ignore the impact on ISW properties of brine drainage from the upper SIPL as it is incorporated into the sea ice by the freezing up of interstitial water, driven by heat loss to the atmosphere. Including such processes would require coupling with a sea ice model such as that of Buffo et al. (2018) mentioned above. Nevertheless, the SS of T_{SC}^{0} calculated using VM and VU models are 0.56 and 0.58, respectively, and the CC and RMSE are also reasonable (Table 2). There are only small differences throughout the time series of T_{SC}^{0} simulated by the VM and VU models (Fig. 4) and the final distributions of both total ISW plume thickness and supercooled thickness are also very similar (see Fig. 5a-d). A comprehensive comparison of T_{SC}^{0} calculated by the VM and VU models in an extensive set of sensitivity experiments will be discussed later. Finally, it can be seen that in both models the ISW plume flow is predominantly governed by a geostrophic balance (Fig 5a-d).

In contrast, the frazil concentration (red lines in Fig. 4b, Fig. 5e and f) and SIPL thickness (green lines in Fig. 4b, Fig. 6b and c) are both underestimated by the VU model, compared with the results of the VM model, throughout the time series. Given the small differences in T_{SC}^{0} calculated by VM and VU models, this result demonstrates that the vertical distribution of frazil concentration within the ISW plume plays a critical role in determining the suspended frazil ice growth (Fig. 2), and thus the frazil concentration and SIPL thickness distributions. The supercooling is utilized more efficiently in the VM model, giving a greater depth-averaged frazil concentration than is produced by the commonly-used VU model. The simulated SIPL thickness near the ISW outflow exhibits steeper gradients than are observed (Fig. 6b and c), which probably result from the spatial non-uniformity of ISW plume near the outflow (Fig. 5a and b). That non-uniformity in flow leads to localized non-uniformities in thermodynamics (Fig. 5c and d), frazil concentration (Fig. 5e and f), and thus SIPL thickness (Fig. 6b and c). Moreover, because the sea ice base is horizontal, there are no changes in the freezing point associated with pressure change, so supercooling is always highest at the ISW outflow (Fig. 5c and d). That results in the greatest frazil concentration (Fig. 5e and f) and SIPL thickness (Fig. 6b and c) near the location of the outflow, and because the outflow is steady in time spatial gradients in SIPL close to the outflow are enhanced. In reality, temporal changes in the ISW outflow position, width, supercooled layer thickness and duration could lead to a broader region of elevated frazil precipitation and a less peaked distribution of SIPL thickness. In addition, such small-scale features in the SIPL thickness distribution, if present, would not be resolved by the relatively coarse spatial distribution of drill-hole measurements (dots in Fig. 6). Nevertheless, the largest SIPL thickness undoubtedly occurs adjacent to the ISW outflow in McMurdo Sound, and the SIPL thickness calculated by the VM model at drill sites agrees well with the measurements (Fig. 6a), being graded "excellent" in contrast with the "poor" performance of the VU model (Table 2). Despite efforts to tune the VU model to give a better match with the observed SIPL thickness, even a limited expansion of SIPL can only be achieved with a considerable increase in the calculated T_{SC}^{0}, in disagreement with the observations.

For both VM and VU models, the time series of area-averaged T_{SC}^{0}, C_i (hereafter T_{SC}^{0} and C_i denote their area-average values), and SIPL thickness indicate respectively two near-constant values and one near-constant growth rate after about the 150th day (Fig. 4b). It is informative to explore how our various assumptions about the vertical distribution of frazil concentration influence the steady-state relationship between those variables in the McMurdo Sound region.

4.2 Dependence of SIPL thickening rate on ISW supercooling

The response of ice shelf basal melting to variations in ocean temperature has been investigated using satellite altimetry (Rignot and Jacobs, 2002; Shepherd et al., 2004) and numerical models (Grosfeld and Sandhäger, 2004; Holland et al., 2008; Payne et al., 2007; Walker and Holland, 2007; Williams et al., 1998, 2002). In contrast, we know of no studies to date that provide a quantitative relationship between marine ice (or SIPL) thickening rate beneath ice shelves (or sea ice) and ISW supercooling. Such a relationship is of potential significance for evaluating the mass balance of deep-draughting ice shelves in cold water environments and adjacent sea ice subject to climatic variability.

Owing to the number of poorly-constrained parameters in the frazil-ice-laden ISW plume model, we conducted 211 comparative sensitivity experiments between VM and VU models, varying both physical and input parameters, including drag coefficient, frazil ice crystal size configuration, average number of frazil crystals, ambient current speed, width and thickness of the ISW outflow, and frazil concentration within the outflow (see Table 3). For all model runs, we plot the relationship between T_{SC}^{0} and thickening rate in the steady state, using output from the last 30 days of each run (Fig. 7).

In Fig. 7a, the results of the VM model are grouped by the prescribed supercooled layer thickness D_{SC}^{ini} in the ISW outflow. For D_{SC}^{ini} <65 m there is a relatively consistent increase in thickening rate with increasing T_{SC}^{0}, while for D_{SC}^{ini} ≥65 m the thickening rate tends to be much more variable. It is worth mentioning that D_{SC}^{ini} =65 m is the value estimated by HU14 based on the measurements conducted by Lewis and Perkin (1985) and Jones and Hill (2001). For D_{SC}^{ini} =78 m and greater, inflexions emerge separating a region of low thickening rate, where the thickening rate tends to decrease with increasing T_{SC}^{0}, from a region of high thickening rate, where there is a very rapid increase in thickening rate with increasing T_{SC}^{0}. This complex response of the VM model must result from the consideration of vertical structure in the frazil concentration, controlled by the frazil ice suspension index Z_* (Fig. 2), in the calculation of frazil ice growth.

We therefore calculated the weighted-average of Z_* at each grid point for the VM model using the following equation:

$$\overline{Z}_* = \frac{\sum_{k=1}^{n} C_i^k Z_*^k}{\sum_{k=1}^{n} C_i^k} = \frac{\sum_{k=1}^{n} C_i^k Z_*^k}{C_i},$$

where C_i^k is the frazil concentration of the kth size class, and n is the number of size classes used. Then, we took the average of $\overline{Z}_*$ over all the grid points occupied by the plume to give a representative suspension index for the VM runs (hereinafter $\overline{Z}_*$ denotes its area-averaged value). We replotted the VM model results characterized by $\overline{Z}_*$ in Fig. 7b. We find systematic changes in $\overline{Z}_*$ with increasing thickening rate (along the coloured lines in Fig. 7b), particularly for D_{SC}^{ini} ≥78 m where the inflexions emerge. With decreasing $\overline{Z}_*$, T_{SC}^0 first decreases, and then increases. If $\overline{Z}_*$ is sufficiently large, the suspended frazil crystals deposit out of the ISW plume so rapidly that they cannot efficiently use the ISW supercooling to grow, leading to the smallest SIPL production for the VM model. For smaller $\overline{Z}_*$, the frazil crystals bathed in the supercooled layer of the ISW plume can remain in suspension and grow longer, resulting in a thicker SIPL and less residual supercooling. However, if $\overline{Z}_*$ decreases further, higher frazil concentration occurs within the lower, overheated part of the ISW plume, where melting of the crystals can mitigate the release of latent heat (Fig. 2b). That promotes further growth of frazil ice which can remain in suspension even longer, and thus lead to rapid SIPL production. The thickening rate calculated by the VU model is also shown, and is discernibly smaller than that calculated by the VM model. In addition, the maximum values of T_{SC}^0 were obtained within the VU model, because the supercooling is used less efficiently for producing SIPL in the VU than in the corresponding VM runs.

These arguments can be further illustrated by a more detailed comparison of T_{SC}^0 calculated by the VM and VU models (Fig. 8). There are a number of runs, including the standard run, that have larger T_{SC}^0 values in the VM than in the VU model. The trend from larger T_{SC}^0 in the VM model to larger T_{SC}^0 in the VU model is accompanied by increases in $\overline{Z}_*$. When $\overline{Z}_*$ is relatively small, large frazil concentration exists within the lower overheated part of the ISW plume (Fig. 2b) where melting of frazil ice (causing cooling) counteracts the consumption of supercooling by frazil growth (causing warming) in the upper part of the plume. As $\overline{Z}_*$ increases, the frazil concentration within the lower overheated part decreases, and finally vanishes, and the resulting release of supercooling in the upper part is more efficient in the VM model, giving larger T_{SC}^0 values in the VU model.

In Fig. 7a, when D_{SC}^{ini} <65 m, ISW supercooling is insufficient to distinguish runs with different $\overline{Z}_*$. In other words, the relation between thickening rate and T_{SC}^0 is independent of $\overline{Z}_*$ for such small D_{SC}^{ini}. When D_{SC}^{ini} is within the range of 65 to 78 m, the VM model results are distinguishable, with data points having smaller thickening rate and larger T_{SC}^0 corresponding to larger $\overline{Z}_*$ (Fig. 7b). When D_{SC}^{ini} ≥78 m, the inflexions emerge, and the ISW supercooling revives when $\overline{Z}_*$ decreases further. Therefore, we conclude that when D_{SC}^{ini} exceeds a critical value (about 65 m for these McMurdo Sound simulations), the efficiency of converting ISW supercooling into frazil ice growth is controlled by the suspension index.

4.3 Dependence of frazil concentration on ISW supercooling

In view of the correlation between SIPL thickening rate and frazil concentration shown in Eq. (3) (also see Fig. 5e and f; Fig. 6b and c), we will explore the relationship between T_{SC}^0 and C_i here. As expected, the complex response of C_i to variations in T_{SC}^0 (Fig. 9) is similar to the relationship between T_{SC}^0 and thickening rate (Fig. 7) in the VM model.

The magnitude of the difference in C_i calculated by VM and VU models (VM minus VU) is compared in Fig. 10a, where we find that C_i calculated by the VM model is always larger than that calculated by the VU model. In general, the difference increases with decreasing $\overline{Z}_*$, while the sensitivity grows with increasing D_{SC}^{ini}. The dependence on $\overline{Z}_*$ is once again due to the impact of the combined thermodynamic processes, i.e., the efficient growth in the upper supercooled part of the plume together with the maintenance of supercooling by melting of frazil in the lower part, discussed above. We also see similar behavior for the difference in the thickening rate (Fig. 10b).

Fig. 7 (Fig. 9) suggests a possible relationship between SIPL thickening rate (frazil concentration) and supercooling in McMurdo Sound, but observations of suspended frazil ice crystal sizes and turbulence within the ISW would be needed to calculate a representative suspension index. To date, there are limited observations of frazil ice in situ, and the majority of the observations made use of instruments not specifically designed for ice crystal detection (Leonard et al., 2006).

5 Summary and future works

In this study, we demonstrated how the vertical distributions of supercooling and frazil ice concentration within an ISW plume jointly determine the growth of suspended frazil ice, and thus the rate of SIPL formation under sea ice and marine ice beneath ice shelves. A vertically-modified, frazil-ice-laden, ISW plume model which encapsulates these combined nonlinear effects was applied to the McMurdo Sound region, and reproduced the observed ISW supercooling and SIPL distributions in two horizontal dimensions. Using multiple model runs, the relationship of ISW supercooling to SIPL thickening rate and frazil concentration in McMurdo Sound was explored, and shown to be dependent on the suspension index that controls the vertical distribution of frazil concentration within the ISW plume. Moreover, when the thickness of a supercooled layer of ISW is large enough, the efficiency of converting ISW supercooling into frazil concentration, and thus SIPL growth is determined by the suspension index. These findings highlight the need for further observations in McMurdo Sound, particularly focused near the ISW outflow region in the western sound, where the supercooled ISW plume and SIPL are prominent, and more general observations that help to constrain the frazil size spectrum within the sea ice-ocean boundary layer. In addition, the performance of the VM model in providing reliable estimates of supercooling and frazil ice flux at the SIPL base makes it an attractive tool for coupling with sea ice models focusing on microscale processes within the bottom layer of the ice (Buffo et al., 2018).

It would be straightforward for the next step to investigate the relationship between supercooling and marine ice thickening rate underneath ice shelves using the VM model. Quantifying this relationship would be the key to parameterizing the process in more complex three-dimensional, primitive equation ocean models, which frequently neglect details of the ice shelf-ocean boundary layer and processes associated with an evolving suspension of frazil ice crystals (Liu et al., 2017, 2018; Mueller et al., 2012, 2018). Results may differ from those discussed above, because of the subtly different environments beneath sea ice and ice shelves. Beneath a SIPL, supercooling is produced by the pressure drop experienced by ISW as it emerges from beneath an ice shelf and rises towards the sea surface, while supercooling that drives marine ice accretion beneath ice shelves is produced as the ISW ascends a very gentle basal slope. The in-situ supercooling level beneath ice shelves is therefore likely to be much smaller than that observed in McMurdo Sound, while the differing slopes also yield differing buoyancy forcing on the flow. Furthermore, after experiencing the step-change in pressure as it ascends the ice front, the supercooled plume in McMurdo Sound is in the process of adjustment, through the formation of suspended frazil and direct freezing onto the accreted SIPL, towards an equilibrium that is presumably attained beyond the region of observations. At the base of an ice shelf, typically several hundred meters thick, the vertical temperature gradient is comparatively small, so the deposited crystals form a slushy layer (Engelhardt and Determann, 1987) that slowly consolidates, possibly as much through compaction as freezing. The ice-ocean interface and the associated drag coefficient are therefore likely to be very different to those observed in McMurdo Sound, where SIPL appears to comprise a more open matrix of ice and water that consolidates by freezing as heat is lost to the atmosphere. In addition, the vastly different time scales over which crystal accretion occurs (about 1-3 years in McMurdo Sound vs tens-hundreds of years beneath ice shelves) could lead to further differences in the internal structure of the crystal layers and hence in the physical boundaries they present to the ISW plume. Therefore, the VM model would need to be re-evaluated against observations of sub-ice shelf ISW plumes and the ice shelf-ocean boundary layer. Finally, further process studies, including the influence of the vertical current structure within either the ice shelf or sea ice -ocean boundary layer (Jenkins, 2016; Robinson et al., 2017) could also contribute to improving our understanding of marine ice and SIPL formation.

Data availability. The data archive associated with this study can be found in the Global Change Master Directory under the keyword K063_2011_2012_NZ_1.

Author contributions. CC led the study. The simulations were designed by ZW and CC, implemented by CL and RX, and analyzed by CC, AJ, and PRH. The paper was written by CC, AJ, and PRH.

Competing interests. The authors declare that they have no conflict of interest.

Acknowledgements. We would like to thank three anonymous referees and Ken Hughes for their thorough review and helpful comments and suggestions. This work was funded by the National Natural Science Foundation of China (41406214, 41876220, 41306208, 41606217). CC and CL were respectively supported by the China Scholarship Council (201708320046, 201504180026). ZW was supported by "the Fundamental Research Funds for the Central Universities" (2017B04814, 2017B20714).

References

Arrigo, K. R., Mock, T., and Lizotte, M. P.: Primary producers and sea ice, Sea ice, 2, 283-325, 2010.

Bombosch, A. and Jenkins, A.: Modeling the formation and deposition of frazil ice beneath Filchner-Ronne Ice Shelf, J. Geophys. Res.-Oceans, 100, 6983-6992, http://doi.org/10.1029/94JC03224, 1995.

Buffo, J. J., Schmidt, B. E., and Huber, C.: Multiphase Reactive Transport and Platelet Ice Accretion in the Sea Ice of McMurdo Sound, Antarctica, J. Geophys. Res.-Oceans, 123, 324-345, https://doi.org/10.1002/2017JC013345, 2018.

Cheng, C., Song, Z. Y., Wang, Y. G., and Zhang, J. S.: Parameterized expressions for an improved Rouse equation, Int. J. Sediment Res., 28, 523-534, http://doi.org/10.1016/S1001-6279(14)60010-X, 2013.

Cheng, C., Huang, H., Liu, C., and Jiang, W.: Challenges to the representation of suspended sediment transfer using a depth-averaged flux, Earth Surf. Proc. Land, 41, 1337-1357, http://doi.org/10.1002/esp.3903, 2016.

Cheng, C., Wang, Z., Liu, C., and Xia, R.: Vertical Modification on Depth-Integrated Ice Shelf Water Plume Modeling Based on an Equilibrium Vertical Profile of Suspended Frazil Ice Concentration, J. Phys. Oceanogr., 47, 2773-2792, http://doi.org/10.1175/JPO-D-17-0092.1, 2017.

Dempsey, D. E., Langhorne, P. J., Robinson, N. J., Williams, M. J. M., Haskell, T. G., and Frew, R. D.: Observation and modeling of platelet ice fabric in McMurdo Sound, Antarctica, J. Geophys. Res.-Oceans, 115, https://doi.org/10.1029/2008JC005264, 2010.

Engelhardt, H. and Determann, J.: Borehole evidence for a thick layer of basal ice in the central Ronne Ice Shelf, Nature, 327, 318–319, https://doi.org/10.1038/327318a0, 1987.

Fricker, H. A., Popov, S., Allison, I., and Young, N.: Distribution of marine ice beneath the Amery Ice Shelf, Geophys. Res. Lett., 28, 2241-2244, https://doi.org/10.1029/2000GL012461, 2001.

Galton-Fenzi, B. K., Hunter, J. R., Coleman, R., Marsland, S. J., and Warner, R. C.: Modeling the basal melting and marine ice accretion of the Amery Ice Shelf, J. Geophys. Res.-Oceans, 117, http://doi.org/10.1029/2012JC008214, 2012.

Gow, A. J., S. F. Ackley, J. W. Govoni, and W. F. Weeks: Physical and structural properties of land-fast sea ice in McMurdo Sound, Antarctica, in Antarctic Sea Ice: Physical Processes, Interactions and Variability, Antarct. Res. Ser., vol. 74, edited by M. O. Jeffries, pp. 355–374, AGU, Washington, D. C., https://doi.org/10.1029/AR074p0355, 1998.

Gough, A. J., Mahoney, A. R., Langhorne, P. J., Williams, M. J., Robinson, N. J., and Haskell, T. G.: Signatures of supercooling: McMurdo Sound platelet ice, J. Glaciol., 58, 38-50, https://doi.org/10.3189/2012JoG10J218, 2012.

Grosfeld, K. and Sandhäger, H.: The evolution of a coupled ice shelf–ocean system under different climate states, Global Planet. Change, 42, 107-132, http://doi.org/10.1016/j.gloplacha.2003.11.004, 2004.

Herraiz-Borreguero, L., Allison, I., Craven, M., Nicholls, K. W., and Rosenberg, M. A.: Ice shelf/ocean interactions under the Amery Ice Shelf: Seasonal variability and its effect on marine ice formation, J. Geophys. Res.-Oceans, 118, 7117-7131, https://doi.org/10.1002/2013JC009158, 2013.

Holland, P. R. and Feltham, D. L.: Frazil dynamics and precipitation in a water column with depth-dependent supercooling, J. Fluid Mech., 530, 101-124, https://doi.org/10.1017/S002211200400285X, 2005.

Holland, P. R. and Feltham, D. L.: The effects of rotation and ice shelf topography on frazil-laden ice shelf water plumes, J. Phys. Oceanogr., 36, 2312-2327, https://doi.org/10.1175/JPO2970.1, 2006.

Holland, P. R., Feltham, D. L., and Jenkins, A.: Ice shelf water plume flow beneath Filchner-Ronne Ice Shelf, Antarctica, J. Geophys. Res.-Oceans, 112, https://doi.org/10.1029/2006JC003915, 2007.

Holland, P. R., Jenkins, A., and Holland, D. M.: The response of ice shelf basal melting to variations in ocean temperature, J. Climate, 21, 2558-2572, https://doi.org/10.1175/2007JCLI1909.1, 2008.

Holland, P. R., Corr, H. F., Vaughan, D. G., Jenkins, A., and Skvarca, P.: Marine ice in Larsen ice shelf, Geophys. Res. Lett., 36, https://doi.org/10.1029/2009GL038162, 2009.

Hughes, K. G., Langhorne, P. J., Leonard, G. H., and Stevens, C. L.: Extension of an Ice Shelf Water plume model beneath sea ice with application in McMurdo Sound, Antarctica, J. Geophys. Res.-Oceans, 119, 8662-8687, https://doi.org/10.1002/2013JC009411, 2014.

Hunkeler, P. A., Hoppmann, M., Hendricks, S., Kalscheuer, T., and Gerdes, R.: A glimpse beneath Antarctic sea ice: Platelet layer volume from multifrequency electromagnetic induction sounding, Geophys. Res. Lett., 43, 222-231, https://doi.org/10.1002/2015GL065074, 2016.

Jenkins, A.: A simple model of the ice shelf–ocean boundary layer and current, J. Phys. Oceanogr., 46, 1785-1803, http://doi.org/10.1175/JPO-D-15-0194.1, 2016.

Jenkins, A. and Bombosch, A.: Modeling the effects of frazil ice crystals on the dynamics and thermodynamics of ice shelf water plumes, J. Geophys. Res.-Oceans, 100, 6967-6981, http://doi.org/10.1029/94JC03227, 1995.

Jones, S. J. and Hill, B. T.: Structure of sea ice in McMurdo Sound, Antarctica, Ann. Glaciol., 33, 5-12, http://doi.org/10.3189/172756401781818347, 2001.

Joughin, I. and Padman, L.: Melting and freezing beneath Filchner-Ronne Ice Shelf, Antarctica, Geophys. Res. Lett., 30, http://doi.org/10.1029/2003GL016941, 2003.

Langhorne, P. J., Hughes, K. G., Gough, A. J., Smith, I. J., Williams, M. J. M., Robinson, N. J., Stevens, C. L., Rack, W., Price, D., Leonard, G. H., Mahoney, A. R., Haas, C., Haskell, T. G.: Observed platelet ice distributions in Antarctic sea ice: An index for ocean-ice shelf heat flux, Geophys. Res. Lett., 42, 5442-5451, https://doi.org/10.1002/2015GL064508, 2015.

Lewis, E. L. and Perkin, R. G.: The winter oceanography of McMurdo Sound, Antarctica, Oceanology of the Antarctic continental shelf, 145-165, https://doi.org/10.1029/AR043p0145, 1985.

Leonard, G. H., Purdie, C. R., Langhorne, P. J., Haskell, T. G., Williams, M. J. M., and Frew, R. D.: Observations of platelet ice growth and oceanographic conditions during the winter of 2003 in McMurdo Sound, Antarctica, J. Geophys. Res.-Oceans, 111, https://doi.org/10.1029/2005JC002952, 2006.

Liu, C., Wang, Z., Cheng, C., Xia, R., Li, B., and Xie, Z.: Modeling modified Circumpolar Deep Water intrusions onto the Prydz Bay continental shelf, East Antarctica, J. Geophys. Res.-Oceans, 122, 5198-5217, http://doi.org/10.1002/2016JC012336, 2017.

Liu, C., Wang, Z., Cheng, C., Wu, Y., Xia, R., Li, B., and Li, X.: On the Modified Circumpolar Deep Water Upwelling Over the Four Ladies Bank in Prydz Bay, East Antarctica, J. Geophys. Res.-Oceans, 123, 7819-7838, https://doi.org/10.1029/2018JC014026, 2018.

Luo, Z., Zhu, J., Wu, H., and Li, X.: Dynamics of the sediment plume over the Yangtze Bank in the Yellow and East China Seas, J. Geophys. Res.-Oceans, 122, 10073-10090, https://doi.org/10.1002/2017JC013215, 2017.

McCave, I. N. and Swift, S. A.: A physical model for the rate of deposition of fine-grained sediments in the deep sea, Geological Society of America Bulletin, 87, 541-546, https://doi.org/10.1130/0016-7606(1976)87<541:APMFTR>2.0.CO;2, 1976.

Morgan, V. I.: Oxygen isotope evidence for bottom freezing on the Amery Ice Shelf, Nature, 238, 393, https://doi.org/10.1038/238393a0, 1972.

Morse, B. and Richard, M: A field study of suspended frazil ice particles, Cold Reg. Sci. Technol., 55, 86-102, https://doi.org/10.1016/j.coldregions.2008.03.004, 2009.

Mueller, R. D., Hattermann, T., Howard, S. L., and Padman, L.: Tidal influences on a future evolution of the Filchner–Ronne Ice Shelf cavity in the Weddell Sea, Antarctica, The Cryosphere, 12, 453, http://doi.org/10.5194/tc-12-453-2018, 2018.

Mueller, R. D., Padman, L., Dinniman, M. S., Erofeeva, S. Y., Fricker, H. A., and King, M. A.: (2012), Impact of tide-topography interactions on basal melting of Larsen C Ice Shelf, Antarctica, J. Geophys. Res.-Oceans, 117, C05005, https://doi.org/10.1029/2011JC007263, 2012.

Oerter, H., Kipfstuhl, J., Determann, J., Miller, H., Wagenbach, D., Minikin, A., and Graft, W.: Evidence for basal marine ice in the Filchner–Ronne Ice Shelf, Nature, 358, 399, https://doi.org/10.1038/358399a0, 1992.

Padman, L. and Erofeeva, S.: Tide Model Driver (TMD) Manual, Version 1.2, Earth and Space Research, Seattle, Wash., 2005. [Available at www.esr.org/polar_tide_models/README_TMD.pdf, last accessed 7 Nov. 2012.]

Payne, A. J., Holland, P. R., Shepherd, A. P., Rutt, I. C., Jenkins, A., and Joughin, I.: Numerical modeling of ocean-ice interactions under Pine Island Bay's ice shelf, J. Geophys. Res.-Oceans, 112, http://doi.org/10.1029/2006JC003733, 2007.

Ralston, D. K., Geyer, W. R., and Lerczak, J. A.: Structure, variability, and salt flux in a strongly forced salt wedge estuary, J. Geophys. Res.-Oceans, 115, C06005, https://doi.org/10.1029/2009JC005806, 2010.

Rees Jones, D. W. and Wells, A. J.: Frazil-ice growth rate and dynamics in mixed layers and sub-ice-shelf plumes, The Cryosphere, 12, 25-38, http://doi.org/ 10.5194/tc-12-25-2018, 2018.

Rignot, E. and Jacobs, S. S.: Rapid bottom melting widespread near Antarctic ice sheet grounding lines, Science, 296, 2020-2023, http://doi.org/10.1126/science.1070942, 2002.

Rignot, E., Jacobs, S., Mouginot, J., and Scheuchl, B.: Ice-shelf melting around Antarctica, Science, 341, 266-270, https://doi.org/10.1126/science.1235798, 2013.

Robinson, N. J., Stevens, C. L., and McPhee, M. G.: Observations of amplified roughness from crystal accretion in the sub-ice ocean boundary layer, Geophys. Res. Lett., 44, 1814-1822, https://doi.org/10.1002/2016GL071491, 2017.

Robinson, N. J., Williams, M. J., Stevens, C. L., Langhorne, P. J., and Haskell, T. G.: Evolution of a supercooled Ice Shelf Water plume with an actively growing subice platelet matrix, J. Geophys. Res.-Oceans, 119, 3425-3446, https://doi.org/10.1002/2013JC009399, 2014.

Shepherd, A., Wingham, D., and Rignot, E.: Warm ocean is eroding West Antarctic ice sheet, Geophys. Res. Lett., 31, http://doi.org/10.1029/2004GL021106, 2004.

Smedsrud, L. H. and Jenkins, A.: Frazil ice formation in an ice shelf water plume, J. Geophys. Res.-Oceans, 109, http://doi.org/10.1029/2003JC001851, 2004.

Smith, I. J., Langhorne, P. J., Haskell, T. G., Trodahl, H. J., Frew, R., and Vennell, M. R.: Platelet ice and the land-fast sea ice of McMurdo Sound, Antarctica, Ann. Glaciol., 33, 21-27, http://doi.org/10.3189/172756401781818365, 2001.

Song, D. and Wang, X. H.: Suspended sediment transport in the Deepwater Navigation Channel, Yangtze River Estuary, China, in the dry season 2009: 2. Numerical simulations, J. Geophys. Res.-Oceans, 118, 5568-5590, http://doi.org/10.1002/jgrc.20411, 2013.

Stern, A. A., Dinniman, M. S., Zagorodnov, V., Tyler, S. W., and Holland, D. M.: Intrusion of warm surface water beneath the McMurdo Ice Shelf, Antarctica, J. Geophys. Res.-Oceans, 118, 7036-7048, https://doi.org/10.1002/2013JC008842, 2013.

Svensson, U. and Omstedt, A.: Numerical simulations of frazil ice dynamics in the upper layers of the ocean, Cold Reg. Sci. Technol., 28, 29-44. http://doi.org/ 10.1016/S0165-232X(98)00011-1, 1998.

Walker, R. T. and Holland, D. M.: A two-dimensional coupled model for ice shelf–ocean interaction, Ocean Model., 17, 123-139, http://doi.org/10.1016/j.ocemod.2007.01.001, 2007.

Williams, M. J. M., Warner, R. C., and Budd, W. F.: The effects of ocean warming on melting and ocean circulation under the Amery Ice Shelf, East Antarctica, Ann. Glaciol., 27, 75-80, http://doi.org/10.3189/1998AoG27-1-75-80, 1998.

Williams, M. J. M., Warner, R. C., and Budd, W. F.: Sensitivity of the Amery Ice Shelf, Antarctica, to changes in the climate of the Southern Ocean, J. Climate, 15, 2740-2757, http://doi.org/10.1175/1520-0442(2002)015<2740:SOTAIS>2.0.CO;2, 2002.

Table 1: List of parameters used in standard model run.

Parameter	Value	Description
f	-1.4244×10^{-4} s^{-1}	Coriolis parameter
$D_{ini}\left(D_{SC}^{ini}\right)$	78 m	Constant ISW plume outflow thickness (constant outflow supercooled layer thickness)
W_{ini}	3 km	ISW plume outflow width with constant $D_{ini}\left(D_{SC}^{ini}\right)$
C_i^{ini}	1×10^{-6}	Depth-averaged volumetric frazil concentration in outflow
N_{ice}	5	Number of frazil ice sizes
$r_{i,1}, r_{i,2}, r_{i,3}, r_{i,4}, r_{i,5}$	0.2, 0.6, 0.9, 1.2, 1.5 mm	Frazil ice radii for each class
a_r	0.02	Aspect ratio of frazil discs
$\bar{n}$	1×10^{3} m^{-3}	Average number of frazil crystals in all size classes per unit volume
C_d	0.02	SIPL basal drag coefficient
V_a	-0.01 m s^{-1}	Ambient flow speed
A_H	100 m^2 s^{-1}	Horizontal eddy viscosity
K_H	20 m^2 s^{-1}	Horizontal turbulent diffusivity
S_{ini}	34.59 psu	ISW plume outflow salinity
T_{ini}	$-0.0573\times S_{ini}+0.0832-7.61\times10^{-4}D_{ini}$	Potential temperature of ISW plume outflow
θ_i	0.075	Shields criterion number

Table 2: List of calculated skill metrics for the results of VM and VU standard model runs.

Variable	RMSE		CC		SS	
	VM	VU	VM	VU	VM	VU
T_{SC}^{0}	0.0070 ºC	0.0069 ºC	0.83	0.84	0.56	0.58
SIPL thickness	1.034 m	2.928 m	0.91	0.01	0.79	-0.65

Table 3: Parameter settings for sensitivity runs, indicated by check, colour-coded by ISW outflow thickness (bottom row). All other parameters remain as they were for the standard model run.

		Drag coefficient				
		0.015	0.0175	0.02	0.0225	0.025
Frazil size configuration (mm)	A: (0.2,0.6,0.9,1.2,1.5)	✓✓✓✓✓✓✓✓		✓✓✓✓✓✓✓✓		✓✓✓✓✓✓✓✓
	1.125×A		✓✓✓✓✓✓✓		✓✓✓✓✓✓✓	
	1.25×A		✓✓✓✓✓✓✓		✓✓✓✓✓✓✓	
	1.375×A		✓✓✓✓✓✓✓		✓✓✓✓✓✓✓	
	1.5×A	✓✓✓✓✓✓✓✓		✓✓✓✓✓✓✓✓		✓✓✓✓✓✓✓✓
	1.625×A		✓✓✓✓✓✓✓		✓✓✓✓✓✓✓	
	1.75×A		✓✓✓✓✓✓✓		✓✓✓✓✓✓✓	
	1.875×A		✓✓✓✓✓✓✓		✓✓✓✓✓✓✓	
	2×A	✓✓✓✓✓✓✓✓		✓✓✓✓✓✓✓✓		✓✓✓✓✓✓✓✓
W_{ini}-ISW plume outflow width with constant $D_{ini}(D_{SC}^{ini})$	1 km			✓✓✓✓✓✓✓		
	5 km			✓✓✓✓✓✓✓		
C_i^{ini}-Depth-averaged volumetric frazil concentration in outflow	0.2×10^{-6}			✓✓✓✓✓✓✓		
	5×10^{-6}			✓✓✓✓✓✓✓		
V_a-Ambient flow speed	0			✓✓✓✓✓✓✓		
	-0.02 m s^{-1}			✓✓✓✓✓✓✓		
$\bar{n}$-Average number of frazil crystals in all size classes per unit volume	200 m^{-3}			✓✓✓✓✓✓✓		
	5000 m^{-3}			✓✓✓✓✓✓✓		

$D_{ini}(D_{SC}^{ini})(m)$−Constant ISW plume outflow thickness (constant outflow supercooled layer thickness)	✓	✓	✓	✓	✓	✓	✓	✓
	30	50	65	70	78	95	100	110

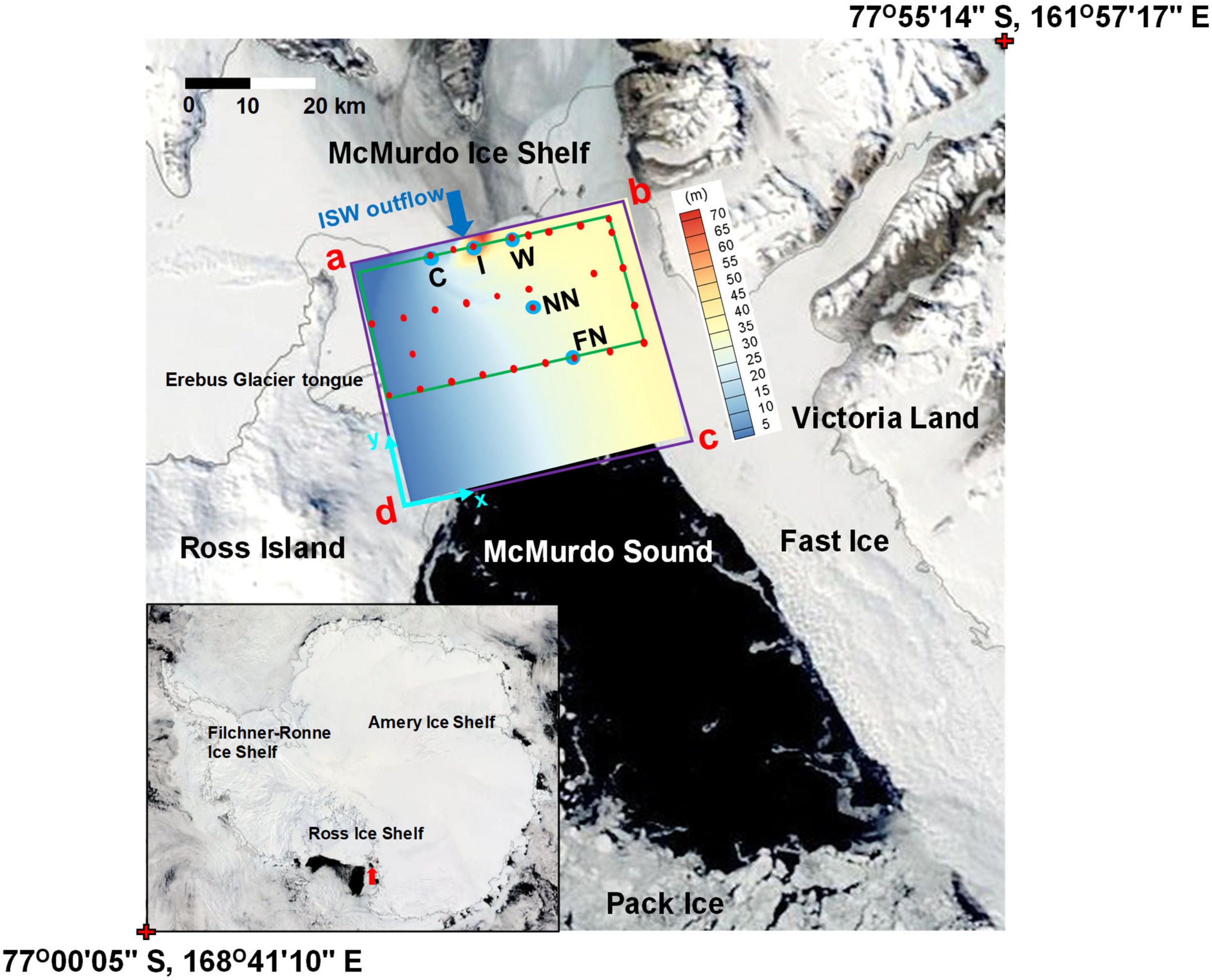

Figure 1: Satellite image of McMurdo Sound region on 29 Nov. 2011. Purple and green frames outline the model and ice borehole (Fig. 6) domains, respectively. Colours within the purple frame indicate the steady state supercooled ISW plume thickness calculated by the vertically-modified ISW plume model in the standard run (Fig. 5d). Light gray lines outline McMurdo Ice Shelf front and coastlines. Model boundaries d-a, a-b (except the ISW outflow) and "b-c" are treated as solid walls, while "c-d" is an open boundary. Blue and red dots respectively mark the oceanographic CTD and ice drilling sites, and the blue arrow represents the location of the ISW outflow in the model. The red arrow in the inset (bottom-left) points to the location of the McMurdo Sound region. Location names C, I, W, NN, and FN mean Central, Intermediate, West, Near North, and Far North, respectively. Satellite image: NASA Rapid Response MODIS Subsets (http://earthdata.nasa.gov/data/near-real-time-data/rapidresponse/modis-subsets).

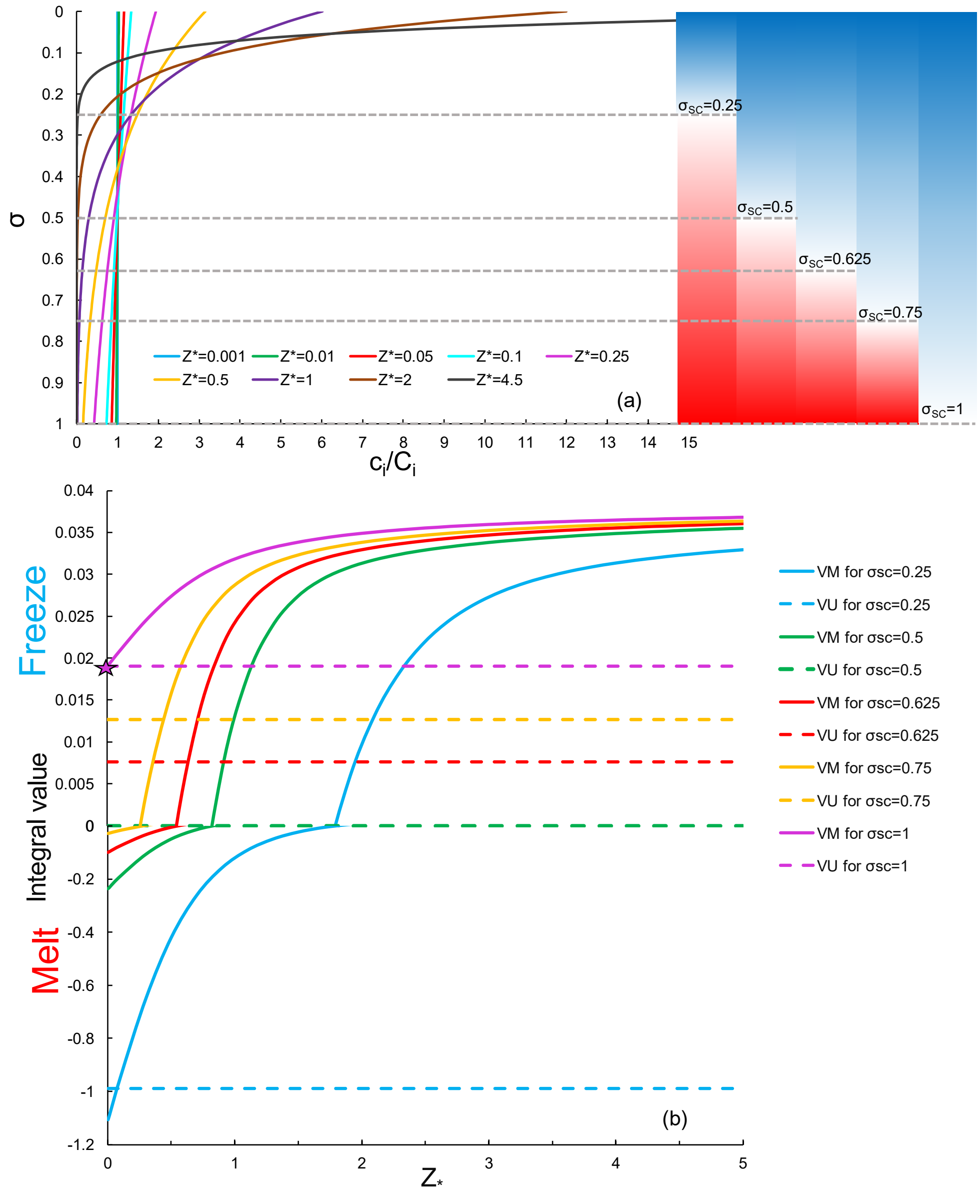

Figure 2: (a) Exponential profiles of equilibrium frazil concentration for selected values of Z_*. Coloured bars at the right and horizontal dashed lines indicate the distribution of supercooling (blue, $T_{SC} > 0$)and overheating (red, $T_{SC} < 0$) for the values of σ_{SC} used in (b). (b) Dependence of integral value of I_{gr} on Z_* for suspended frazil ice freezing ($I_{gr} > 0$) and melting ($I_{gr} < 0$) under the supercooling conditions shown in (a). The star denotes the particular conditions under which the integral values of I_{gr} calculated using VU and VM formulations are equal. Note that different y-axis scales are used for freezing and melting.

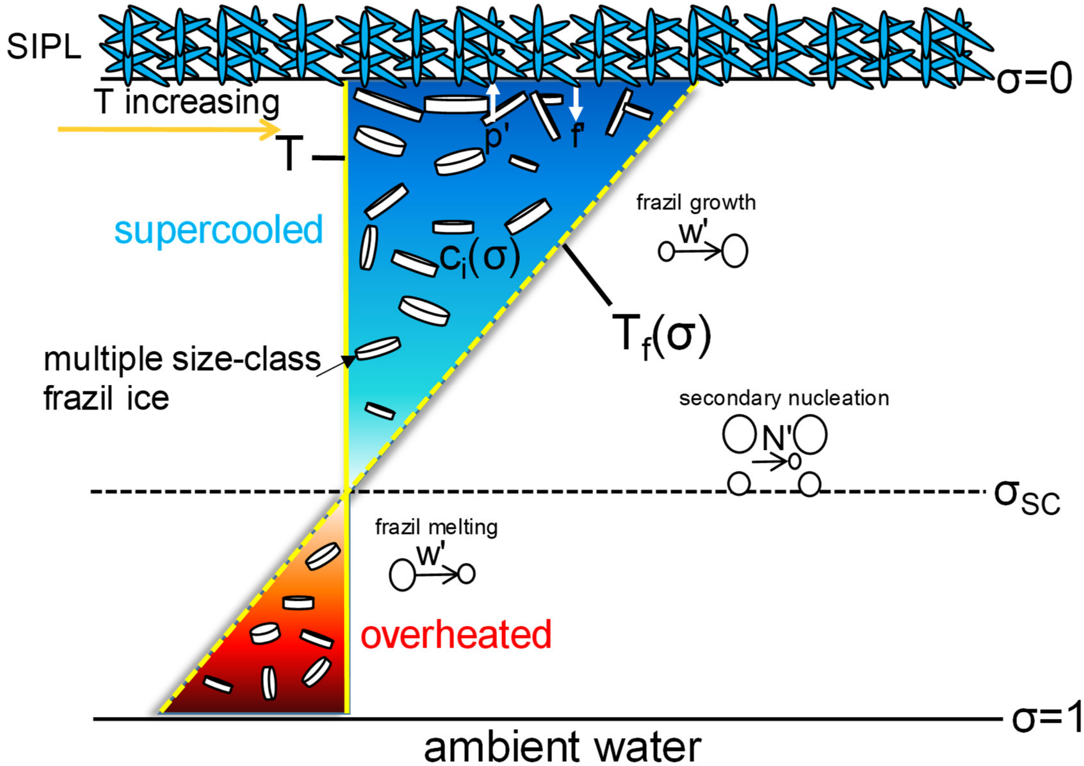

Figure 3: Schematic diagram of vertical distribution of thermal forcing and relevant processes within a supercooled ISW plume of homogeneous potential temperature and salinity. Secondary nucleation is the process by which the frazil ice in the smallest class is supplemented by collisions between other larger frazil ice crystals.

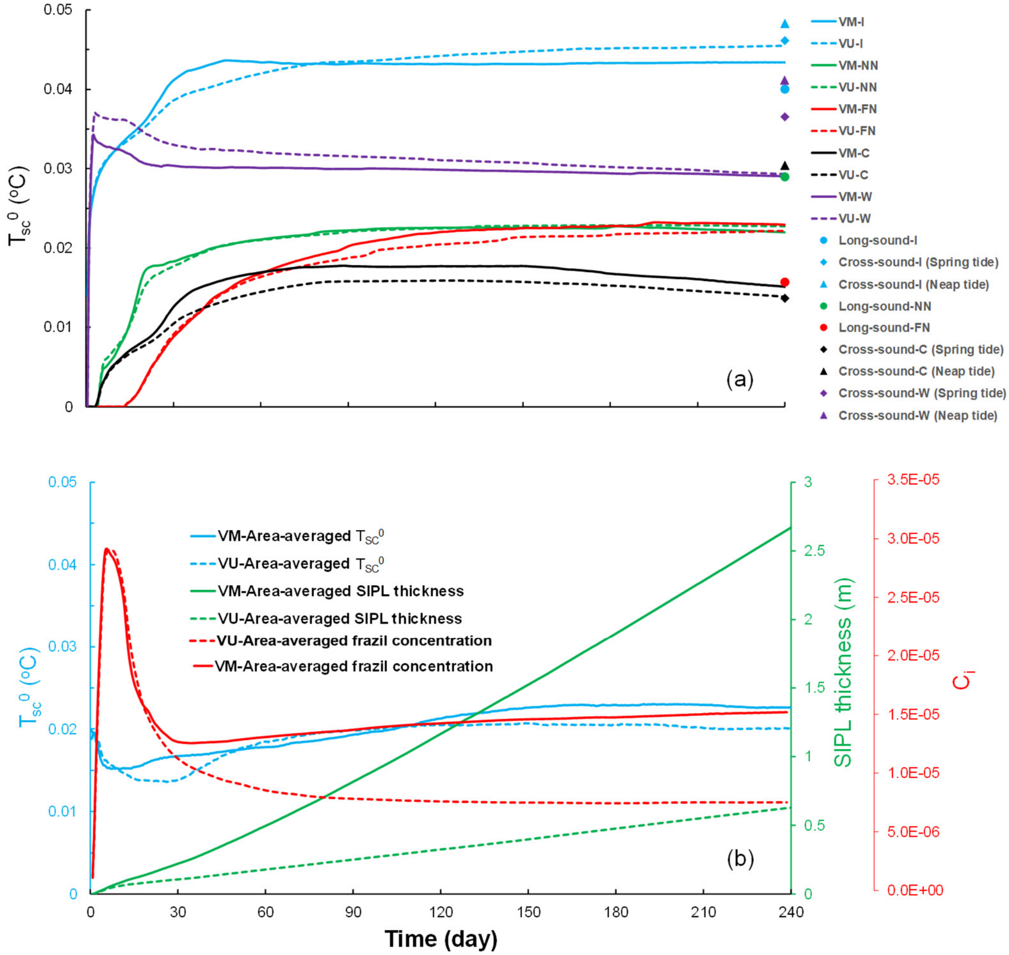

Figure 4: (a) Time series of T_{SC}^0 simulated by VM (solid lines) and VU (dashed lines) models at five oceanographic sites (colour-coded) in the McMurdo Sound region. (b) Time series of area-averaged T_{SC}^0 (blue), SIPL thickness (green), and frazil concentration (red) simulated by VM (solid lines) and VU (dashed lines) models over the model domain (purple frame in Fig. 1).

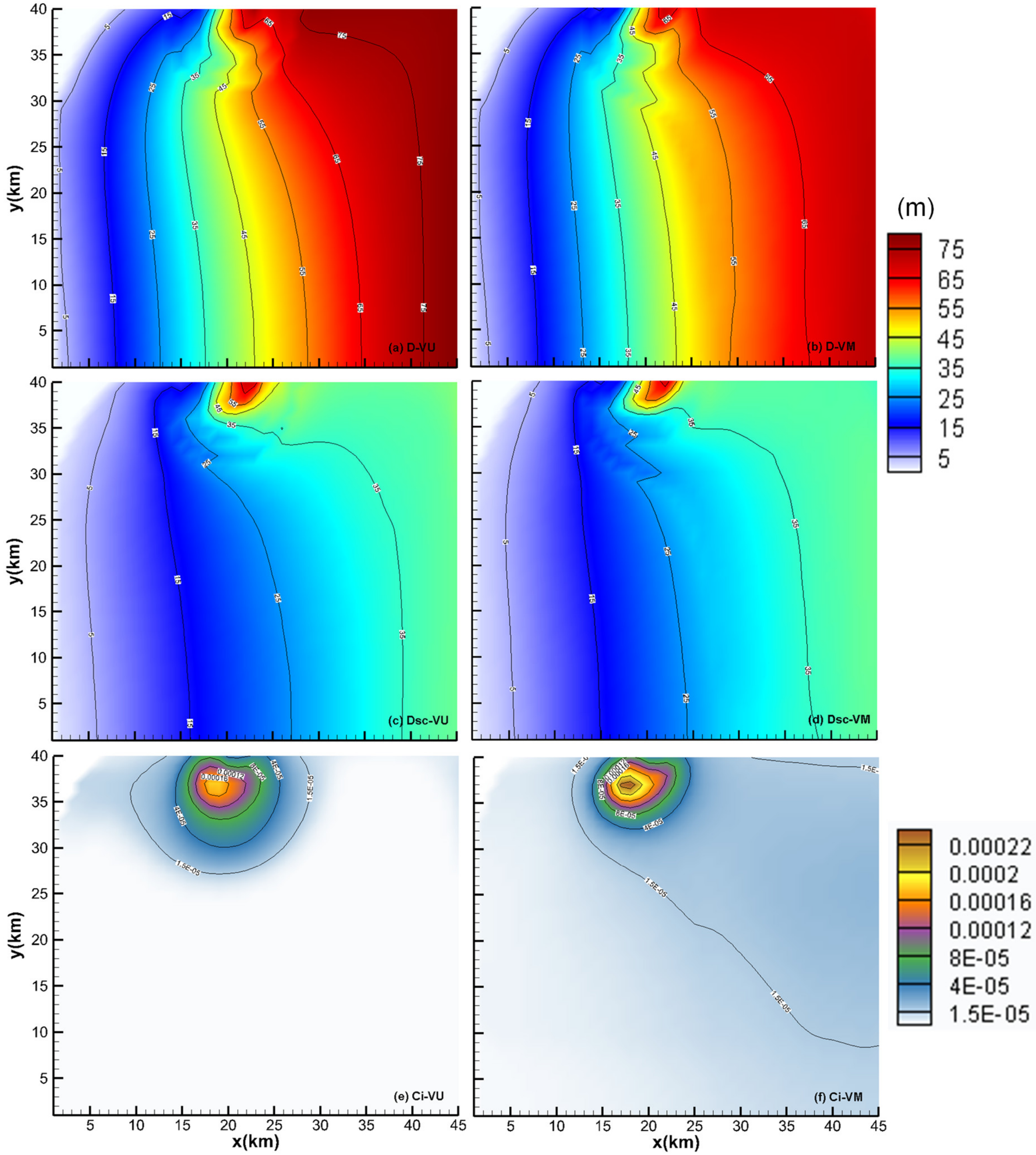

Figure 5: Spatial patterns, interpolated from model results using Natural Neighbour method, of (a), (b) total, (c), (d) supercooled ISW plume thickness, and (e), (f) depth-averaged frazil concentration at the end of the standard runs of (a), (c), (e) VU and (b), (d), (f) VM models over the domain (purple frame in Fig. 1). Note that the colour scale used in (a-d) is unified.

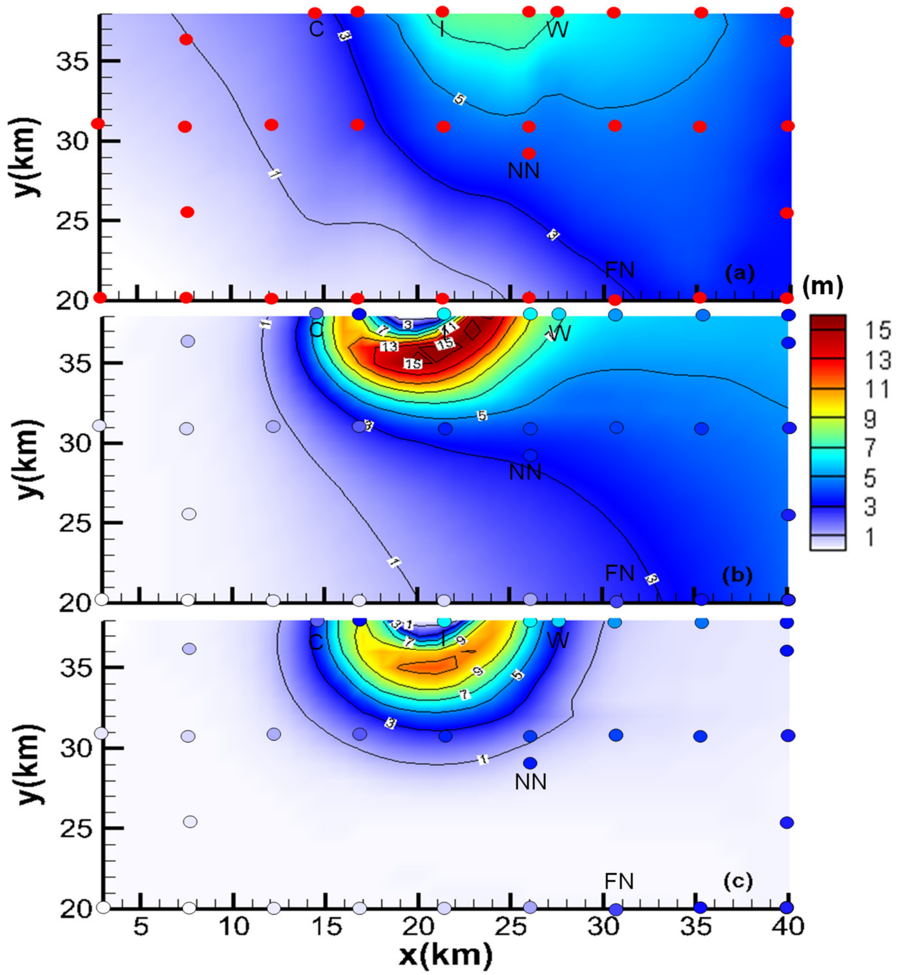

Figure 6: (a) SIPL thickness over green box in Fig. 1 interpolated, using Natural Neighbor method, from drill-hole measurements (red dots). (b) and (c) SIPL thickness derived from (b) VM and (c) VU models, compared with drill-hole measurements (colour-coded dots). Note that the colour scale is unified.

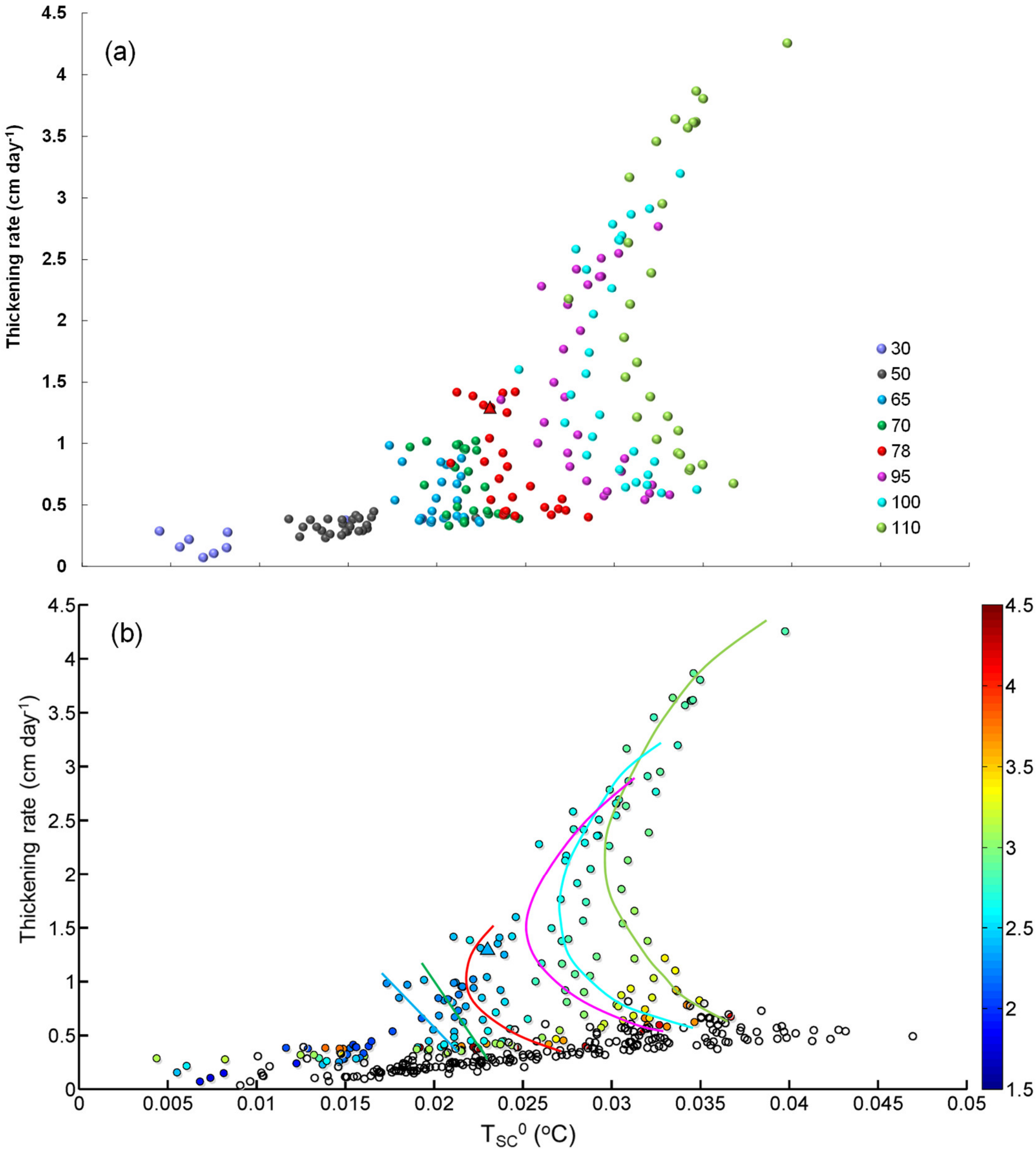

Figure 7: Relationship between T_{SC}^{0} and thickening rate classified by (a) outflow supercooled layer thickness D_{SC}^{ini} and (b) $\overline{Z_*}$ (colour-coded). Numbers in legend of (a) represent the values of D_{SC}^{ini}. Solid and hollow dots in (b) correspond to the VM and VU model runs, respectively. Coloured lines depict the central trend of the corresponding data points shown in (a). Triangle corresponds to the standard run. The results are from the last 30 days of the model runs.

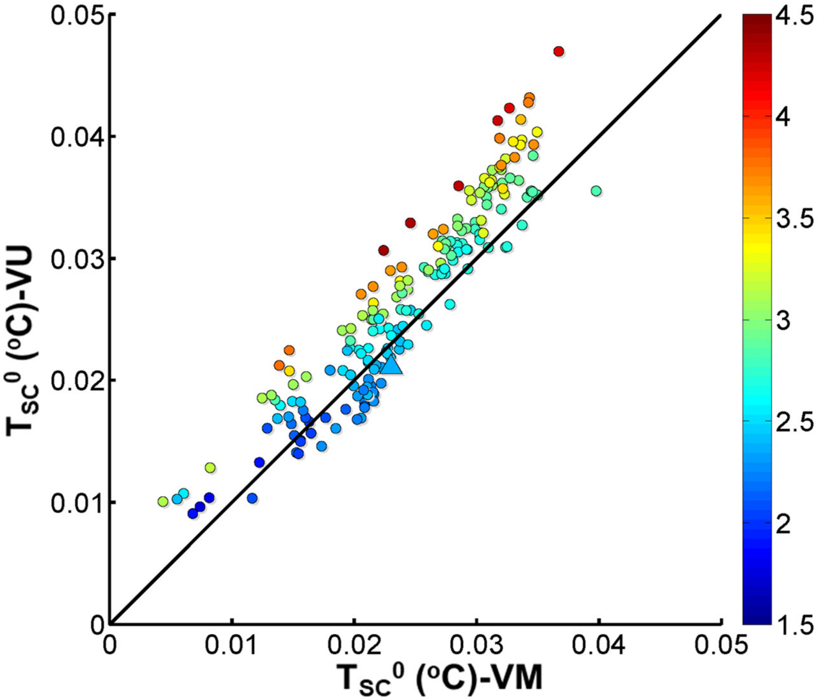

Figure 8: Comparison of T_{SC}^{0} calculated by the VM and VU models. Triangle corresponds to the standard run. The colour scale of $\overline{Z_*}$ is the same as in Figure 7b.

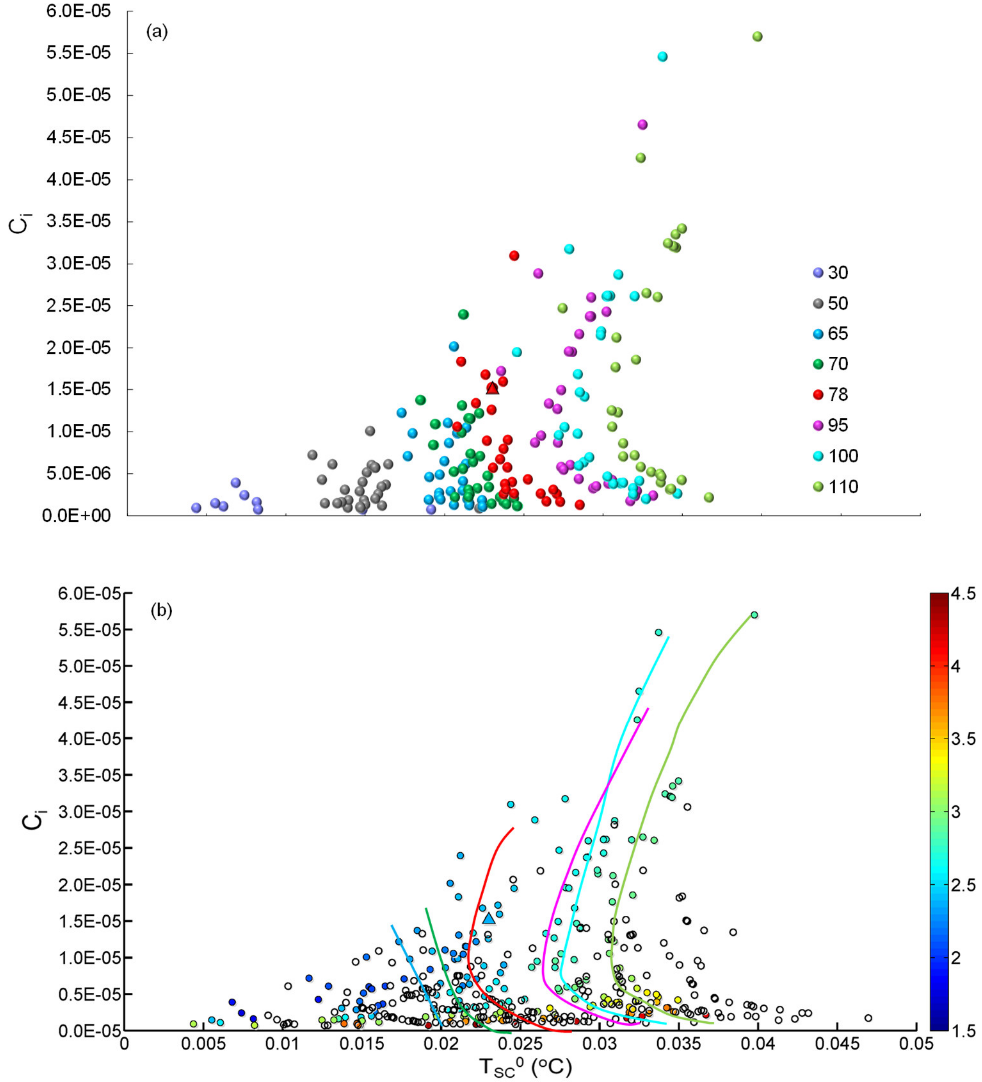

Figure 9: Same as Fig. 7, but for the relationship between T_{SC}^{0} and C_i.

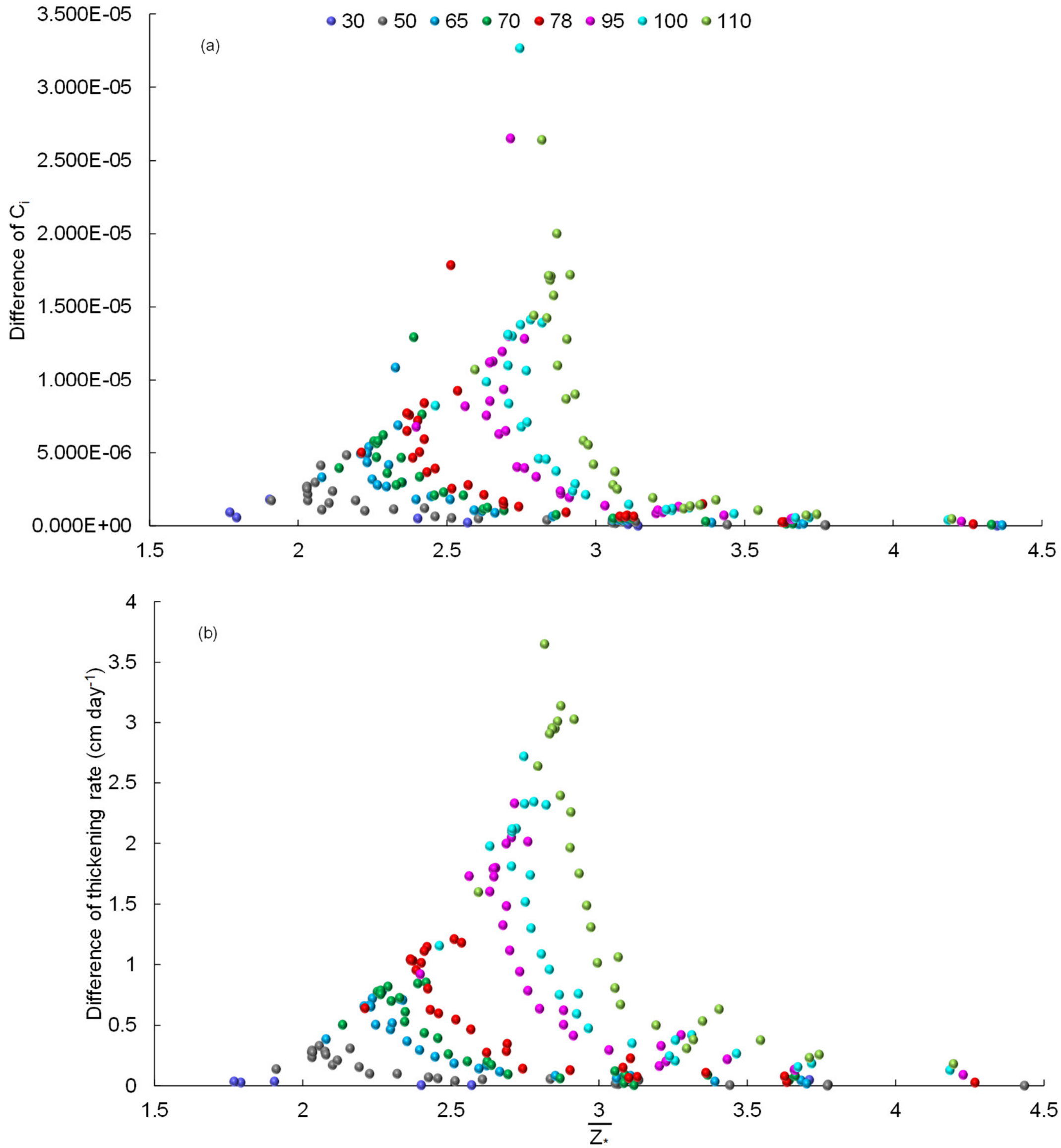

Figure 10: Relationship between $\overline{Z_*}$ and difference of (a) C_i and (b) thickening rate calculated by VM and VU models (VM minus VU), classified by outflow supercooled layer thickness D_{SC}^{ini}. Numbers in legend represent the values of D_{SC}^{ini}.